ISBN 978-82-326-3916-8 (printed version)
ISBN 978-82-326-3917-5 (electronic version)

Doctoral theses at NTNU, 2019:159

Martin Bakken

Transient analysis of wet gas compressor systems

NTNU
Norwegian University of
Science and Technology
Faculty of Engineering
Department of Energy and Process Engineering

NTNU
Norwegian University of
Science and Technology

Doctoral theses at NTNU, 2019:159

NTNU

NTNU
Norwegian University of
Science and Technology

Martin Bakken

Transient analysis of wet gas compressor systems

Thesis for the degree of Philosophiae Doctor

Trondheim, June 2019

Norwegian University of Science and Technology
Faculty of Engineering
Department of Energy and Process Engineering

NTNU
Norwegian University of
Science and Technology

NTNU
Norwegian University of Science and Technology

Thesis for the degree of Philosophiae Doctor

Faculty of Engineering
Department of Energy and Process Engineering

ISBN 978-82-326-3916-8 (printed version)
ISBN 978-82-326-3917-5 (electronic version)

Doctoral theses at NTNU, 2019:159

Printed by Skipnes Kommunikasjon as

ABSTRACT

The demand for oil and gas remains high, and changing market conditions require innovative solutions. Development of compression technology tailored for subsea oil and gas production can contribute significantly to profitability of both new and existing fields. Installation close to the well-head assures enhanced extraction and extended operation from gas/condensate fields. Additional benefits are: Exploitation of more remote fields, increased process simplicity and profitable extraction from fields with lower wellhead pressures.

Wet gas compression is challenging due to the complex behavior of multiphase flows, which impacts the thermodynamics and fluid dynamics of the compression process. Moreover, subsea compressor systems demand high availability owing to the difficulty and cost related to maintenance. Hence, knowledge regarding compressor behavior in transient conditions is pivotal to maintain production.

In the present work, attention has been given to wet gas compressor system behavior in transient conditions. The work presented here is a combination of experimental research and model simulation. The majority of the experimental research is obtained from a single-stage centrifugal compressor operating in air/water flow, located at the Norwegian University of Science and Technology (NTNU). The test facility is an open loop configuration operating at ambient conditions. A dynamic process simulation model has been built to replicate the test facility and to conduct detailed engineering studies.

The main objective of the work has been to contribute to development of the dynamic simulation tool, to include modeling of wet gas compressors. Accurate and applicable modeling techniques are important with respect to design and operation of wet gas compressor systems.

The experimental results reveal that the pressure ratio increases and the polytropic efficiency decreases when the compressor is subjected to wet gas flow. Care should be taken when analyzing stability and surge margins at different gas mass fractions (GMFs). Further, the interaction between the impeller, diffuser and volute is vital to understand with respect to compressor performance and stability.

The compressor performance has been analyzed when subjected to inlet slugs down to a GMF of 0.185, which imposed a marked impact on the gas flow rate, compressor shaft torque and compressor pressure ratio.

The wet gas impact on the control valve performance has been studied and analyzed. The results reveal that wet gas not only alters the compressor performance, but also the system behavior. The combined effect is important to understand for development and operation of future wet gas compressor systems.

In cooperation with Aspentech R&D, Hysys Dynamics has been extended to support modeling of wet gas compressors. This enables the user to input multiple performance curves at different GMFs as well as different compressor speeds. The compressor performance methodology has been validated when operating with several wet performance curves. Further, the applicability of the affinity laws in wet conditions has been studied. Finally, the simulation model has been validated against several transient test cases and provided a close correspondence to these.

Continued studies should involve the influence of different multiphase flow characteristics on the compressor and system performance. Further studies on flow behavior through the impeller and diffuser would also be of great interest, and potentially give insight into new design principles. Based on my work a redesign of the volute is suggested to physically remove the possibility of volute backflow.

More studies are necessary to continue development of wet gas compressor modeling, i.e. additional parameters, like the fluid density ratio, are needed to accommodate the performance shift related to changes in composition and inlet conditions. Finally, emphasis should be given to system behavior and system response to contribute to design and operation of future subsea production systems.

ACKNOWLEDGEMENTS

I began my studies as a PhD-student on wet gas compression in 2016. This has been an experience which I have greatly enjoyed. I have had the opportunity and pleasure to conduct extensive experimental research at the NTNU wet gas compressor research facility. The work has allowed me to participate in several international technical conferences.

It has been truly inspiring to contribute to this novel field of technology together with some of the foremost experts in the field. Main supervisor Tor Bjørge's versatile knowledge regarding compressor dynamics and practical engineering has been very helpful. Thanks to Professor Lars Eirik Bakken for his flexibility and guidance during my studies. Øyvind Hundseid deserves a thanks for valuable consultation during this work. I would also like to thank Professor Ole Gunnar Dahlhaug for rewarding advice and dialogues regarding the scope of work. A big thank you to Erik Langørgen, for his sound experimental expertise and versatility. His persistency and utility have been essential to document the experimental findings presented in this thesis.

I want to take the opportunity to thank Equinor for their support of the test rig modification and for providing the fundamental research work with valuable challenges related to industrial applications. Equinor's engagement has been a prerequisite for my work. Thanks to Aspentech, with Dr. Ajay Lakshmanan and his team in Boston, for engaging in the collaboration on model simulation of wet gas compressors.

Last but not least, I want to thank my family for their support during all my studies. Special thanks to my girlfriend and cohabitant Merethe Kristiansen for her patience, support, and motivation throughout this work.

LIST OF PAPERS

I. M. Bakken, T. Bjørge, “An experimental investigation on hysteresis in a wet gas compressor”, ASME GTIndia 2017, GTIndia2017-4518.

II. M. Bakken, T. Bjørge, “Volute flow influence on wet gas compressor performance”, ASME GTIndia 2017, GT2017-4529.

III. M. Bakken, T. Bjørge, L.E. Bakken, “Wet gas compressor operation and performance”, IMECE 2018, IMECE2018-86562.

IV. M. Bakken, T. Bjørge, “An experimental investigation on the impact of inlet slugging on wet gas compressor performance”, ASME Turbo Expo 2017, GT2017-65094.

V. M. Bakken, T. Bjørge, L.E. Bakken, A. Lakshmanan, S. Arulselvan, “Wet gas compressor modeling and performance scaling”, ASME Turbo Expo 2019, GT2019-90353.

VI. M. Bakken, T. Bjørge, L.E. Bakken, “Wet gas compressor model validation”, ASME Turbo Expo, GT2019-90354.

VII. M. Bakken, E. Lunde, L.E. Bakken, “Digital Compressor Analytics”, ASME Turbo Expo 2018, GT2018-76583.

TABLE OF CONTENTS

ABSTRACT I
ACKNOWLEDGEMENTS III
LIST OF PAPERS V
TABLE OF CONTENTS VII
LIST OF FIGURES IX
LIST OF TABLES XI
NOMENCLATURE XIII
1 INTRODUCTION 1
1.1 Background 1
1.2 Subsea compression 2
1.3 Dynamic model simulation 2
1.4 Scope of work 3
1.5 Limitations 3
1.6 Thesis outline 3
2 WET GAS COMPRESSION 5
2.1 Wet compressor test facility 5
2.2 Wet gas fundamentals 6
Wet gas parameters 6
Flow characteristics 8
Hysteresis 9
Performance analysis 9
Compressor system 10
3 DYNAMIC PROCESS SIMULATION 13
3.1 Introduction to Hysys Dynamics 13
Integration strategy 13
Holdup model and pressure-flow solver 13
Centrifugal compressor 14
4 EXPERIMENTAL RESULTS AND ANALYSIS 15
4.1 Compressor hysteresis 15
Revised design - Diffuser trim 20
Summary and conclusion 21
4.2 Wet gas compressor performance 21
Summary and conclusion 23
4.3 Inlet slugging on compressor performance 23
Artificial slug 24

Terrain slug 25
Slugging in subsea wet gas compressor systems 25
Summary and conclusion 26
5 SIMULATION RESULTS AND ANALYSIS 27
5.1 Wet gas compressor modeling 27
NTNU dynamic simulation model 27
5.2 Compressor performance methodology and model accuracy 28
Validation against hydrocarbon data 29
Applicability of the affinity laws in wet gas flow 31
Summary and conclusion 32
5.3 Wet gas compressor model validation 33
Driver trip test 33
Gradual increase of liquid content 34
Multiphase valve performance 35
Summary and conclusion 36
5.4 Digitalization of compressor systems 36
Dynamic model results 38
Summary and conclusion 39
6 CONCLUSION 41
7 FURTHER WORK 43
REFERENCES 45
PAPER I 47
PAPER II 48
PAPER III 49
PAPER IV 50
PAPER V 51
PAPER VI 52
PAPER VII 53

LIST OF FIGURES

FIGURE 1: HISTORY AND FORECAST OF OIL AND GAS PRODUCTION ON NCS [2]. 1
FIGURE 2: P&ID OF THE TEST FACILITY 5
FIGURE 3: COMPRESSOR TEST FACILITY 6
FIGURE 4: COMPRESSOR CROSS SECTION....6
FIGURE 5: MULTIPHASE FLOW CHARACTERISTICS IN A HORIZONTAL PIPE 8
FIGURE 6: SYSTEM RESISTANCE CURVE....10
FIGURE 7: SIMPLIFIED SIMULATION NETWORK OF A TYPICAL COMPRESSOR SYSTEM 14
FIGURE 8: COMPRESSOR HYSTERESIS AT GMF 0.95 [10] 15
FIGURE 9: THE DIFFUSER SECTION AND A MONITOR CAPTURING THE COMPRESSOR OPERATING POINT 15
FIGURE 10: COMPRESSOR PERFORMANCE CHARACTERISTICS AT 9000 RPM 15
FIGURE 11: COMPRESSOR PERFORMANCE AND DIFFUSER FLOW REGIME AT GMF A) 1.0 B) 0.901 C) 0.970 D) 0.951 E) 0.921 F) 0.907 G) 0.896 17
FIGURE 12: COMPRESSOR PERFORMANCE FROM GMF 1.0 TO GMF 0.896 18
FIGURE 13: DIFFUSER FLOW TRANSITION FROM GMF 0.991 TO GMF 0.970....18
FIGURE 14: DIFFUSER FLOW TRANSITION FROM GMF 0.970 TO GMF 0.951.....18
FIGURE 15: LIQUID FLOW SWIRLING FROM DIFFUSER HUB- TO SHROUD....19
FIGURE 16: OBSERVED VOLUTE FLOW DIRECTION. 19
FIGURE 17: COMPRESSOR PERFORMANCE GMF 0.975....19
FIGURE 18: COMPRESSOR PERFORMANCE GMF 0.95....19
FIGURE 19: DIFFUSER/VOLUTE FLOW IMPACT ON COMPRESSOR PERFORMANCE AT GMF 0.975 20
FIGURE 20: DIFFUSER/VOLUTE FLOW IMPACT ON COMPRESSOR PERFORMANCE AT GMF 0.95 20
FIGURE 21: COMPRESSOR PERFORMANCE AT GMF 0.975 – REVISED DIFFUSER DESIGN 21
FIGURE 22: COMPRESSOR PERFORMANCE AT GMF 0.95 – REVISED DIFFUSER DESIGN 21
FIGURE 23: COMPRESSOR PRESSURE RATIO CHARACTERISTICS....22
FIGURE 24: POLYTROPIC HEAD AGAINST TOTAL VOLUMETRIC FLOW RATE 22
FIGURE 25: POLYTROPIC EFFICIENCY AGAINST TOTAL VOLUMETRIC FLOW RATE 23
FIGURE 26: TEST ARRANGEMENT FOR ARTIFICIAL SLUG 23
FIGURE 27: TEST ARRANGEMENT FOR TERRAIN SLUG....23
FIGURE 28: ARTIFICIAL SLUG INITIATION – WATER VALVE POSITION AND LIQUID FLOW RATE 24
FIGURE 29: ARTIFICIAL SLUG – COMPRESSOR SPEED AND SHAFT TORQUE 24
FIGURE 30: ARTIFICIAL SLUG – GAS FLOW RATE AND STATIC COMPRESSOR PRESSURE RATIO....24
FIGURE 31: TERRAIN SLUG – DISCHARGE VALVE POSITION AND GAS VOLUME FLOW RATE 25
FIGURE 32: TERRAIN SLUG – COMPRESSOR SPEED AND SHAFT TORQUE....25
FIGURE 33: TERRAIN SLUG - COMPRESSOR SPEED AND STATIC COMPRESSOR PRESSURE RATIO 25
FIGURE 34: COMPRESSOR SYSTEM RESPONSE DURING INLET SLUGGING – INCREASED PERFORMANCE AT REDUCED GMF 26
FIGURE 35: COMPRESSOR SYSTEM RESPONSE DURING INLET SLUGGING – REDUCED PERFORMANCE AT REDUCED GMF 26
FIGURE 36: DYNAMIC SIMULATION MODEL OF THE NTNU TEST FACILITY 28
FIGURE 37: SUDDEN INCREASE OF LIQUID CONTENT AND ITS IMPACT ON COMPRESSOR SPEED 28
FIGURE 38: SUDDEN INCREASE OF LIQUID CONTENT AND ITS IMPACT ON COMPRESSOR SHAFT TORQUE....28
FIGURE 39: POLYTROPIC HEAD VS TOTAL VOLUME FLOW RATE FOR A MULTISTAGE COMPRESSOR OPERATING IN HYDROCARBON FLOW. 29
FIGURE 40: POLYTROPIC EFFICIENCY VS TOTAL VOLUME FLOW RATE FOR A MULTISTAGE COMPRESSOR OPERATING IN HYDROCARBON FLOW. .29
FIGURE 41: THE FLUID DENSITY RATIO IMPACT ON THE PERFORMANCE OF A MULTISTAGE CENTRIFUGAL COMPRESSOR IN HYDROCARBON FLOW. 31
FIGURE 42: COMPRESSOR PERFORMANCE SCALING IN TERMS OF STATIC COMPRESSOR PRESSURE RATIO AND TOTAL VOLUME FLOW RATE....31
FIGURE 43: COMPRESSOR PERFORMANCE SCALING IN TERMS OF POLYTROPIC HEAD AND TOTAL VOLUME FLOW RATE. 31
FIGURE 44: COMPRESSOR PERFORMANCE SCALING IN TERMS OF POLYTROPIC EFFICIENCY AND TOTAL VOLUME FLOW RATE....32
FIGURE 45: TESTED COMPRESSOR PERFORMANCE IN COMPARISON TO THE AFFINITY LAWS....32
FIGURE 46: GMF IMPACT ON COMPRESSOR DECELERATION 33
FIGURE 47: GMF IMPACT ON COMPRESSOR PERFORMANCE DURING TRIP 33
FIGURE 48: COMPRESSOR SPEED DECELERATION – TEST VS SIMULATION 34
FIGURE 49: STATIC COMPRESSOR PRESSURE RATIO – TEST VS SIMULATION 34
FIGURE 50: A STEPWISE INCREASE OF LIQUID CONTENT – TEST VS SIMULATION. 34

FIGURE 51: VALVE INLET FLOW RATE AGAINST VALVE OPENING 35
FIGURE 52: VALVE DIFFERENTIAL PRESSURE AGAINST VALVE OPENING 35
FIGURE 53: MULTIPHASE VALVE FLOW COEFFICIENT 36
FIGURE 54: A STEPWISE INCREASE OF LIQUID CONTENT AT HIGH FLOW RATES WITH - TEST VS SIMULATION 36
FIGURE 55: EXPORT COMPRESSOR SYSTEM. 37
FIGURE 56: TRIP BASED ON MEASURED FLOW AND STATIC PRESSURE READINGS. 37
FIGURE 57: STATIC DISCHARGE PRESSURE READING. 37
FIGURE 58: TRIP TRAJECTORY BASED ON MEASURED COMPRESSOR SPEED, STATIC PRESSURE READINGS AND UTILIZATION OF FAN LAW PRINCIPLES. 38
FIGURE 59: SIMULATED RUNDOWN TRAJECTORY. 38
FIGURE 60: MEASURED VS SIMULATED COMPRESSOR SPEED DURING RUNDOWN. 38
FIGURE 61: MEASURED VS SIMULATED MASS FLOW RATE. 39
FIGURE 62: MEASURED VS SIMULATED MASS FLOW WHEN ACCOUNTING FOR TIME DELAY AND SIGN CONVERSION. 39
FIGURE 63: LABORATORY SETUP FOR FUTURE DIGITAL ANALYSIS. 39

LIST OF TABLES

TABLE 1: MAIN COMPRESSOR DIMENSIONS 5
TABLE 2: INSTRUMENTATION ACCURACY 6
TABLE 3: TEST START CONDITIONS 20
TABLE 4: TEST CONDITION – ARTIFICIAL SLUG 24
TABLE 5: TEST CONDITIONS – TERRAIN SLUG 24
TABLE 6: SIMULATION VS TEST AT GMF 0.95 29
TABLE 7: SIMULATION VS TEST AT GMF 0.90 29
TABLE 8: SIMULATION VS HYDROCARBON PERFORMANCE DATA AT GMF 0.95 30
TABLE 9: SIMULATION VS HYDROCARBON PERFORMANCE DATA AT GMF 0.85 30
TABLE 10: DEVIATION BETWEEN COMPRESSOR PERFORMANCE AND THE AFFINITY LAWS AT BEP. 32

NOMENCLATURE

C_v	Valve flow coefficient	[-]
D	Diameter	[m]
F_p	Piping geometry factor	[-]
GMF	Gas Mass Fraction	[-]
GVF	Gas Volume fraction	[-]
Hp	Polytropic head	[J/kg]
H	Total head	[J/kg]
I	Polar inertia	[kg/m^2]
KE	Kinetic energy	[J]
$\dot{m}$	Mass flow rate	[kg/s]
Ma	Mach number	[-]
n	Polytropic exponent	[-]
Q	Volumetric flow rate	[m^3/s]
p	Static pressure	[bar]
Pr	Static pressure ratio	[-]
P	Power	[W]
R	Gas constant	[J/KgK]
Rh	Relative humidity	[%]
SG	Specific gravity	[-]
St	Stokes number	[-]
T	Temperature	[K]
u	Velocity	[m/s]
v	Specific volume	[m^3/kg]
We	Weber number	[-]
Y	Expansion factor	[-]
Z	Compressibility factor	[-]

Greek

δ	Fluid density ratio	[-]
η_p	Polytropic efficiency	[-]
ρ	Density	[kg/m^3]
σ	Surface tension	[N/m]
τ	Torque	[Nm]
τ_F	Flow field characteristic time	[s]
φ	Flow coefficient	[-]
μ	Viscosity	[kg/ms]
ω	Angular speed	[s^{-1}]

Subscripts

1	Inlet
2	Discharge
A	Initial value
B	Current value
c	Compressor
d	Droplet
g	Gas
l	Liquid
mp	Multiphase
tot	Total

1 INTRODUCTION

This thesis is intended to illuminate how a wet gas compressor system behaves when subjected to transient conditions and to contribute to development of dynamic simulation tools, to model wet gas compressors. The work presented here is a combination of experimental research and model simulation. The majority of the experimental research is obtained from a single-stage centrifugal compressor operating in air/water flow. A dynamic process simulation model has been built to replicate the test facility and to conduct detailed engineering studies.

The purpose of the thesis is to summarize the authors published works and to place them in relation to each other and in context to the technological maturity.

1.1 Background

Oil and gas production on the Norwegian continental shelf (NCS) is expected to increase in the coming years, as shown in Figure 1. The total oil and gas production in 2023 is predicted to be of the same magnitude as the peak production in 2004. This shows that the oil and gas sector is still heavily invested in and necessary to satisfy global energy demands. The 2017 resource report from the Norwegian Petroleum Directorate [1] documents that the current estimates of oil and gas reserves on the NCS, including undiscovered resources, exceed the total accumulated production from 1971.

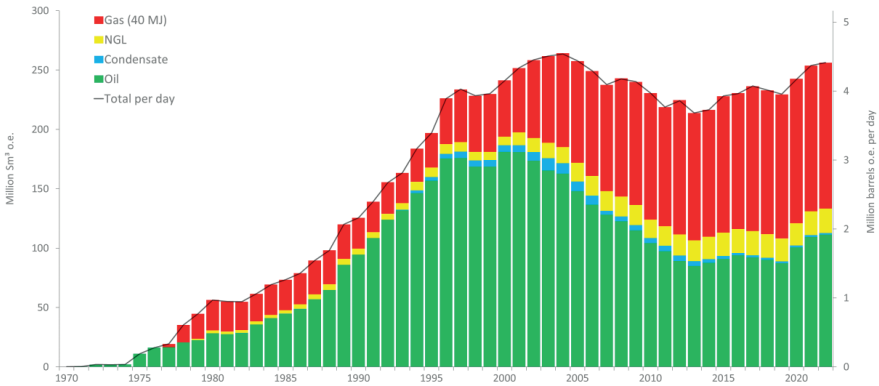

Figure 1: History and forecast of oil and gas production on NCS [2].

Today, existing fields are extending their commercial life expectancy by an average of 12 years from the original development plan, owing to implementation of various production methods and technologies. Future development of oil and gas reserves requires solutions which increase the recovery of both new and existing fields. Several methods are available; some are listed below [1].

- Drilling far more wells than originally planned.
- New or amended drainage strategies and increased reservoir understanding.
- Implementing new technology.
- Expanding infrastructure capacity and flexibility.
- Tying-in third-party fields, which extends producing life and therefore output for the host field.

The ability to continue production at low wellhead pressure represents perhaps the most important method for increasing recovery from existing gas fields. This relies on introduction of additional compressors to boost production pressure. The late life recovery project on the Ormen Lange field represents one of the largest projects involving low-pressure production. The initial stage focused on on-shore compressor boosting. A subsea compression solution is being evaluated for the next phase, which entails pressure-boosting closer to the wellhead and thereby extends production and recovery additionally.

1.2 Subsea compression

Subsea compression may provide the most significant benefit when seeking to increase recovery from existing offshore gas/condensate fields. Other benefits involves production from marginal fields and cost reductions due to unmanned operation [3]. Moreover, direct compression of the well stream represents reduced investment costs owing to process simplicity.

Several compressor designs have been evaluated and developed for wet gas flow. The applicability of the screw compressor was investigated by Müller-Link et al [4] and found to be a feasible design. The contra rotating axial design has been installed subsea on the Gullfaks field in the North Sea, see Knudsen et al [5]. In addition, the centrifugal compressor has made its way into the field of wet gas compression due to its robustness, scalability and long operating history in the oil and gas industry. On the Åsgard field, two subsea compressor modules have been installed based on the centrifugal compressor design. These machines have been equipped with an inlet scrubber to cater for liquid transients, i.e. liquid slugs or "wet surges". Reference is given to Kleynhans et al [6].

Although subsea compression involves considerable benefits, several challenges need to be catered for regarding technology, operation and design of such systems.

- *Design guidelines:* Currently there are no standard design guidelines for process compressors operating in wet gas flow, such as ISO 10439 [7] and API 617 [8] for conventional process compressors. Wet gas flow involves complex multiphase flows and phases with fundamentally different properties, which will interact during compression. Thus, the design guidelines will need some revision to accommodate the influence on both compressor performance and mechanical aspects e.g. erosion.
- *Test codes and correction methods:* The ASME PTC10 [9] performance test code describes the necessary test setup, measurement techniques and accuracy requirements, in addition to the applicable correction methods with respect to operating conditions and fluids. As multiphase flows influence both the thermodynamics and fluid mechanics, the test code cannot be applied to wet gas flow. Hence, development of test codes applicable to wet gas flow is necessary.
- *Transient operation:* Multiphase flow like slug flow or "wet surges" represent one of the major operational challenges for subsea compression systems, as it may impose a devastating impact on the production (system shutdown) and the mechanical integrity of the compressor. Hence, a smart and versatile system design is necessary to cope with multiphase flows. Driver trip in wet conditions, compressor start-up and parallel operation of several compressor trains are examples of other transient scenarios, which demand attention.
- *Production:* Subsea compressor systems demand high availability owing to the difficulty of conducting maintenance. Frequent maintenance on such systems will quickly make the investment unprofitable.

1.3 Dynamic model simulation

Dynamic simulations tools have proven invaluable for numerous applications in the process/chemical industry, including compressor systems. With the stringent availability demands for subsea compression systems, process simulation models are expected to play a pivotal role regarding condition monitoring and system operation. Moreover, such systems will provide key information on scenario based case studies like:

- Driver trip in wet conditions
- System response to inlet slugs
- Compressor start-up
- Detecting compressor degradation and its influence of system response

In order to utilize dynamic process models for wet gas compression systems, development and validation of the tool is required. In cooperation with Aspentech R&D, Hysys Dynamics has been extended to support modeling of wet gas compressors. This enables the user to input multiple performance curves at different gas/liquid content as well as different compressor speeds. In addition, the user has the possibility to input multiple surge and stonewall curves based on the gas mass fraction. The work presented in this thesis includes

validation of the accuracy of the compressor performance procedure when operating with multiple wet performance curves, the applicability of the affinity laws in wet conditions and transient model simulation.

1.4 Scope of work

The current work focuses on both experimental research and model simulation related to transient compressor system behavior in wet gas flow. The main objective of the work has been to contribute to development of the dynamic simulation tool, to include modeling of wet gas compressors. Accurate and applicable modeling techniques are important with respect to design and operation of wet gas compressor systems. The goal of the *experimental work* is summarized below:

- Establish a sound and repeatable compressor performance characteristics in wet gas flow.
- Analyze the compressor system response in transient operating conditions.

Establishment of accurate wet gas performance data is important to validate the functionality and accuracy of the wet gas compressor within Hysys Dynamics. Moreover, the simulated system response is largely dependent on the performance curves. The goal of the *model simulation work* is summarized below:

- Develop a wet gas compressor block within Hysys Dynamics.
- Develop and tune a dynamic simulation model of the NTNU test facility.
- Analyze the applicability of the compressor performance methodology within the model and validate the simulation model against experimental transient test cases.

1.5 Limitations

Wet gas compression involves complex thermodynamics and fluid mechanics, which in turn are altered by the mixture pressure, composition and compressor geometry. A thorough investigation in all these dimensions is considered necessary to gain a comprehensive understanding regarding compressor performance analysis and design principles. The experimental limitations are summarized below:

- *Fluid properties:* The experimental work is primarily based on air/water performance data at ambient conditions. Compared to high pressure natural gas, this poses significant changes in properties such as density ratio, surface tension and mixture viscosity.
- *Compressor design:* The experimental work is primarily limited to a single-stage centrifugal compressor, with a vaneless diffuser and a circular volute.

1.6 Thesis outline

Chapter 1: A general introduction and the scope of work.

Chapter 2: Description of the NTNU wet gas test facility, including introduction to fundamental dimensionless parameters.

Chapter 3: An introduction to dynamic process simulation and the principles of Hysys Dynamics.

Chapter 4: Experimental work and test campaigns.

Chapter 5: Model description, simulation results and test campaigns.

Chapter 6: Conclusion and recommendations for further work.

References

Paper I: An experimental investigation on hysteresis in a wet gas compressor

Paper II: Volute flow influence on wet gas compressor performance

Paper III: Wet gas compressor operation and performance

Paper IV: An experimental investigation on the impact of inlet slugging on wet gas compressor performance

Paper V: Wet gas compressor modeling and performance scaling

Paper VI: Wet gas compressor model validation

Paper VII: Digital compressor analytics

2 WET GAS COMPRESSION

2.1 Wet compressor test facility

The experiments presented in this thesis have primarily been conducted in the wet gas compression research facility located at the Department of Energy and Process Engineering, at NTNU Trondheim. The test facility is an open loop configuration consisting of a shrouded centrifugal impeller, a vaneless diffuser and a symmetrical circular volute. The compressor can be powered up to a maximum rotational speed of 11000 rpm by a 450 kW electric motor. Table 1 shows the main compressor data.

Table 1: Main compressor dimensions

Parameter	Quantity
Impeller outlet diameter	400mm
Diffuser ratio	1.7
Inlet hub diameter	250mm
Outlet pipe diameter	200mm

The instrumentation has been installed in accordance with ASME PTC 10. The experimental fluid is a mixture of ambient air and water. The liquid injection system is installed directly upstream of the compressor and consists of 16 uniformly distributed water injection nozzles. A water pump and a control valve enable a wide range of liquid flow rates. Suction and discharge hydraulic valves enable tuning of the gas flow rate, which is measured by an orifice plate on the compressor suction side. The impeller power requirement is measured by a torque meter installed between the motor rotor and the impeller shaft. The motor is controlled by a Variable Speed Drive (VSD). Figure 2 shows the test rig layout and Table 2 shows the instrumentation accuracy.

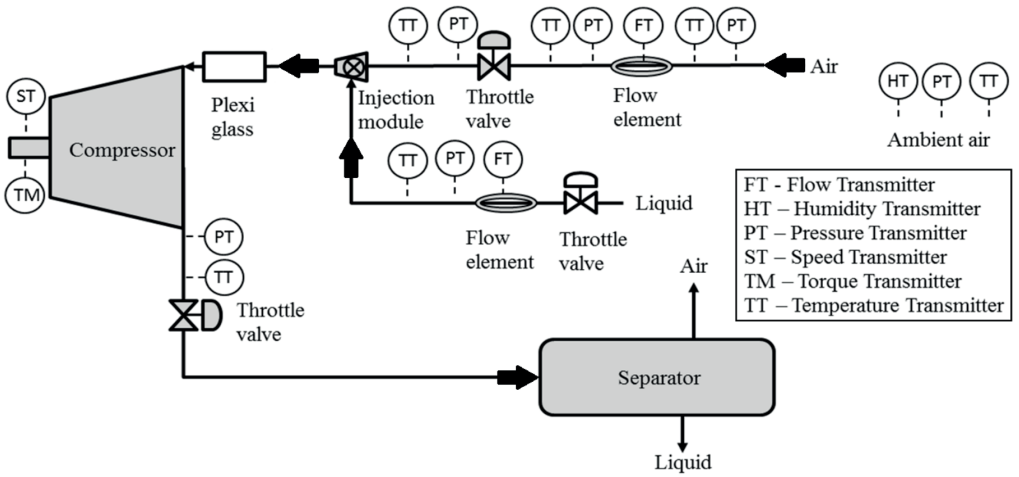

Figure 2: P&ID of the test facility

Table 2: Instrumentation accuracy

Instrument section	*Accuracy*	*Unit*
Ambient temperature	± 0.2	°C
Ambient pressure	± 0.15	hPa
Relative humidity	± 1	%
Temperature flow element	± 0.15	°C
Pressure diff. flow element	± 0.04	%
Dynamic pressure diffuser	0.14	mbar
Static pressure diffuser	0.002	bar
Total temperature diffuser	0.009	°C
Three hole probe diffuser	0.11	%
Inlet pressure compressor	± 0.3	%
Inlet temperature compressor	± 0.005	°C
Outlet pressure compressor	± 0.3	%
Outlet temperature compressor	± 0.006	°C
Water flow meter	± 0.5	%
Shaft speed	± 5	%
Shaft torque	± 0.05	%

The test facility allows both steady and transient testing. The data acquisition system is based on a National Instrument PXI, which ensures time consistent measurements up to 20 kHz. The test facility is depicted in Figure 3, showing the liquid injection manifold and the compressor. Plexiglas has been fitted on the compressor inlet, diffuser and volute section, enabling observation of the multiphase flow characteristics. Figure 4 shows the compressor cross section and the visualization windows. For a more comprehensive test rig description, see Hundseid et al [10].

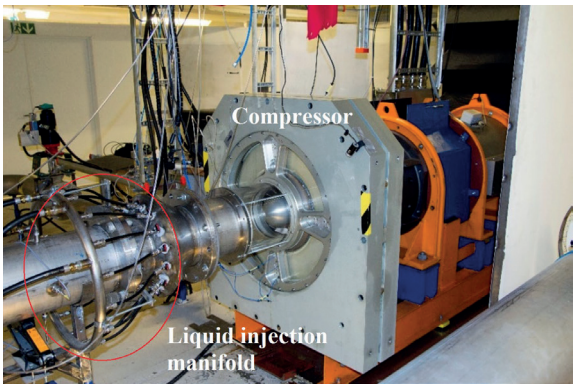

Figure 3: Compressor test facility

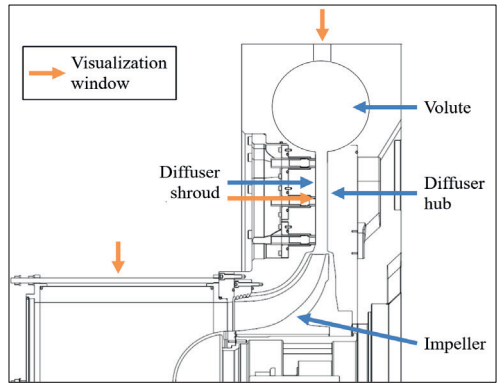

Figure 4: Compressor cross section

2.2 Wet gas fundamentals

This section focuses on the fundamental parameters describing wet gas flow and the influence on centrifugal compressor performance. In addition, wet gas performance analysis, flow characteristics and system behavior are covered here.

Wet gas parameters

A wet gas compressor is considered suitable when exposed to multiphase mixtures with gas content in the range of 95 - 100%, on a volumetric basis. The remaining content is liquid condensate and an aqueous phase. Both the *gas volume fraction* (GVF) and the *gas mass fraction* (GMF) are commonly used to address the amount of gas relative to the total mixture.

$$GVF = \frac{Q_g}{Q_g + Q_l} \tag{1}$$

$$GMF = \frac{\dot{m}_g}{\dot{m}_g + \dot{m}_l} \tag{2}$$

Several authors have published experimental performance data regarding the GMF/GVF impact on centrifugal compressor performance. In 2005, Brenne et al [11] documented the performance of a single-stage centrifugal compressor operating at 50-70 bar, with hydrocarbon gas and condensate as the working fluid. Among several conclusions, they found that increasing liquid content results in a pressure ratio increase, a decrease in the polytropic efficiency and a decrease in the specific compressor power. Bertoneri et al [12] conducted experiments on a two-stage centrifugal compressor operating at 20 bar, with air/water as the experimental fluid. Their work reveals similar findings, i.e. increased liquid content results in a higher compressor pressure ratio, reduced polytropic efficiency and reduced temperature ratio.

The *fluid density ratio* is an important parameter in wet gas flow providing an indication of the multiphase flow behavior and the interaction between the phases. The difference in phase densities has a direct influence on phase separation. Additionally, the fluid density ratio influences critical multiphase parameters like the Stokes and Weber numbers.

$$\delta = \frac{\rho_g}{\rho_l} \tag{3}$$

Limited research has been documented on the density ratio impact on single-stage performance. One of the best references, Hundseid et al [13], shows that changing liquids, from hydrocarbon to water, entails a wet gas performance shift equivalent to going from 70 to 50 bar suction pressure for a hydrocarbon liquid.

The multiphase flow characteristics, i.e. droplet size and breakup, are influenced by both the surface tension and viscosity. The tendency to form liquid film and droplets is linked to the ratio between the fluid kinetic energy and liquid surface tension, described by the *Weber number.* The droplet size has been reported to have varying impact on compressor performance. Brenne et al [11] reported that the droplet size had a limited impact on compressor performance. Fabbrizzi et al [14] on the other hand, documented a distinct performance impact by removing the inlet pipe and injecting a fine spray directly into the inducer.

$$We = \rho_l \frac{u_g^2 D_d}{\sigma_d} \tag{4}$$

Further research on the Weber number impact on flow regime and impeller stage losses, as well as the shift in *Reynolds frictional losses* is required to obtain reliable analysis and prediction tools. However, the fundamental mechanisms of changed multiphase apparent viscosity impact on the multiphase pump performance provide an important knowledge basis and contribution to the wet gas challenges; see Ramberg et al [15].

The Stokes number is a measure of the droplets' ability to respond to velocity changes in the flow field. A small Stokes number (St << 1) indicates that the droplets are able to follow the gas flow field closely whereas a large Stokes number (St >> 1) indicates that the droplets will easily detach from the flow field, especially at sudden turns or during acceleration. Obviously, the Stokes number is an important parameter for turbomachinery operating in two-phase flow, where the fluid needs to be deflected, accelerated and decelerated. Hence, the Stokes number will provide an indication of the droplet deposition and droplet acceleration through the impeller and the deceleration capability of the diffuser.

$$St = \frac{\rho_l D_d^2 / 18 \mu_g}{\tau_F} \tag{5}$$

In-depth study of the wet gas impact on the compressor diffuser flow characteristics, losses and pressure recovery is documented by Brenne et al [16]. The fluid absolute velocity related to the speed of sound, represented by the Mach number, requires further investigation.

Flow characteristics

One of the challenges in subsea wet gas compression (direct compression) involves the difficulty of controlling the liquid content at the compressor inlet. Experience has shown that the liquid content may deviate considerably relative to the average liquid fraction in the well. This is due to several factors including pipe-pressure, diameter and elevation, well composition, gas velocities and fluid properties. Thus, it is of fundamental importance to validate how the liquid content alters the compressor performance and stability. Figure 5 shows how the multiphase flow regime typically changes as functions of gas and liquid flow rates.

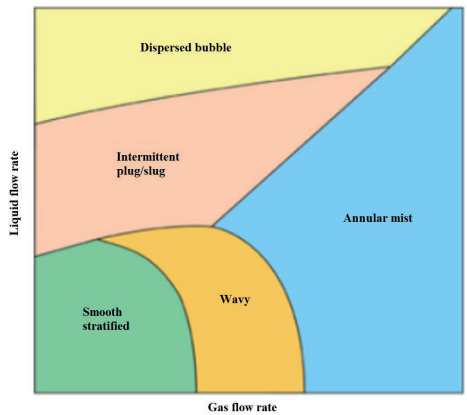

Figure 5: Multiphase flow characteristics in a horizontal pipe

Being able to ensure stable and predictable compressor behavior in subsea installations is challenging. As the reservoir pressure drops during production, the compressor enters a region where it is far more susceptible to inlet slugging. The term “wet surges”, used by the industry may be more suitable, which describe a sudden and substantial increase of liquid content, and not necessarily a liquid plug covering the entire pipe cross section.

Inlet slugging may lead to internal compressor damage, including damage to seals, bearings and compressor blades. Thus, liquid slugs must be catered for with respect to system design and process control. For instance, on Åsgard Subsea Compression there is an added slug volume in the inlet scrubber. This will handle fast changes in liquid load while the pump is speeding up to respond to the added liquid flow.

Determining the ability of the compressor system to handle inlet slugging conditions is pivotal. The energy balance within a compressor and motor system is given by Equation 6. The change in kinetic energy is balanced against the power provided from the drive, fluid power and friction losses.

$$\frac{dKE}{dt} = \frac{d}{dt}\left(\frac{1}{2} I_{tot} \omega_c^2\right) = P_{Drive} - P_{Fluid} - P_{Friction} \tag{6}$$

It is crucial that the drive is able to act swiftly and provide sufficient power during slugs. If it is not, the compressor will inevitably decelerate, which may influence compressor stability and in the worst case lead to compressor surge. Similarities can be drawn to compressor trips where traditionally no power is available from the drive during compressor rundown. McGee et al [17] documented the compressor control system’s impact on the trip trajectory. Tveit et al [18] [19] showed that a high compressor polar inertia and a high head rise to surge are beneficial concerning surge avoidance during trip.

Hysteresis

Hysteresis is an unstable flow phenomenon which may occur in rotating machinery, e.g. centrifugal pumps and compressors. The phenomenon is well-known in the pump industry and involves temporary deviations from the established performance characteristics. In many cases, hysteresis entails increased pressure fluctuations, Stoffel et al [20], and accounts for a significant discontinuity in pressure rise coefficient and pump efficiency, Kaupert et al [21]. Hysteresis normally occurs at low flow rates, typically in the range of 65 – 75% of design flow, as documented by Hergt et al [22], and involves complex three-dimensional flow with recirculation. Fraser et al [23] describe two forms of recirculation, namely suction recirculation involving local backflow at the impeller eye and discharge recirculation entailing local backflow at the impeller discharge. Hence, hysteresis is associated with dynamic impeller loading, flow induced vibrations and cavitation. Unsteady flow phenomena and hysteresis have also been experienced for compressors. Day et al [24] describes hysteresis effects in relation with the onset and cessation of rotating stall.

Performance analysis

International standards, both the ASME PTC10 and ISO5389, are based on Schultz polytropic approach [25] that accounts for real gas behavior. In summary, the approach includes:

$$H_p = \int_1^2 v dp \approx \frac{n}{n-1}[p_2 v_2 - p_1 v_1] \tag{7}$$

The process follows the polytropic compression path specified by $pv^n = Constant$. At given suction and discharge conditions the polytropic volume exponent is defined as:

$$n = \frac{\ln\left(\frac{p_2}{p_1}\right)}{\ln\left(\frac{v_1}{v_2}\right)} \tag{8}$$

The polytropic efficiency and fluid power are defined by:

$$\eta_p = \frac{vdp}{dh} = \frac{H_p}{H} \tag{9}$$

$$P_{fluid} = \frac{\dot{m}_1 H_p}{\eta_p} = \frac{\rho_1 Q_1 H_p}{\eta_p} \tag{10}$$

No standards specify the performance evaluation procedure for *wet gas*. An approach frequently used in the 1990's was based on the *two fluid model* approach, adding the gas and liquid polytropic head requirement:

$$H_{p,mp} = GMF \frac{n}{n-1} Z_1 R T_1 \left(\left(\frac{p_2}{p_1}\right)^{\frac{n-1}{n}} - 1 \right) + (1 - GMF)\left(\frac{p_2 - p_1}{\rho_l}\right) \tag{11}$$

The approach however has several shortcomings, e.g. it does not cover fluid evaporation or condensation between suction and discharge. Going back to the fundamental approach, utilizing the polytropic analysis for any type of fluid, including multiphase fluids, the derivation of the polytropic head remains valid. This is known as the *total fluid approach*, defined by:

$$H_{p,mp} = \frac{n}{n-1}[p_2 v_2 - p_1 v_1] \tag{12}$$

The polytropic efficiency and fluid power remain:

$$\eta_{p,mp} = \frac{vdp}{dh} = \frac{H_{p,mp}}{H_{mp}} \tag{13}$$

$$P_{mp,fluid} = \frac{\dot{m}_{1,mp} H_{p,mp}}{\eta_{p,mp}} = \frac{\rho_{1,mp} Q_{1,mp} H_{p,mp}}{\eta_{p,mp}} \tag{14}$$

The wet gas performance analysis in this thesis is based on the total fluid approach, utilizing equation 12, 13 and 14.

Compressor system

The compressor reacts according to the system. The system consists of all surrounding process equipment, which includes piping, bends, valves, scrubbers, coolers/heaters, safety system and drive. The system imposes a certain resistance, which is captured with the *system resistance curve*. The interaction between the compressor performance curve and the system resistance curve pinpoints the operating point within the performance envelope. Figure 6 illustrates the concept. In addition, slight physical or thermodynamic changes may alter the system resistance curve. This accounts for changes in either pressure, temperature, GMF, composition or velocities.

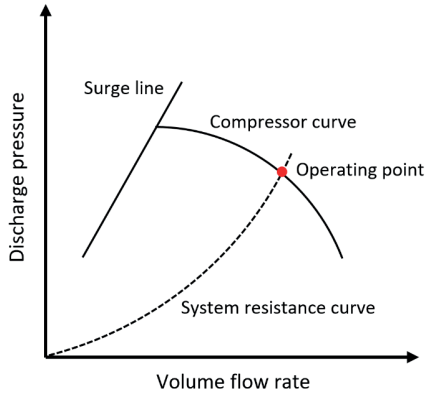

Figure 6: System resistance curve

Another key aspect with respect to compressor operation is the compressor inlet and discharge volumes. Large inlet and discharge volumes will result in a slow pressure convergence towards the new operating conditions. This in turn could be critical in scenarios like compressor or driver trip. The slow pressure response leads to a close to constant compressor pressure ratio during the first few hundred milliseconds after a trip. Simultaneously the speed decreases, forcing the compressor to the left in the characteristics, towards surge. Depending on the action of the safety system, the compressor may recover without entering the surge region of the characteristics. In the case of a driver trip the drive power is cut immediately, leaving the compressor to decelerate only against the fluid power and friction losses (Equation 6).

Driver trip may also be a serious concern for wet gas compression systems. The liquid content contributes to a higher total mass flow, which increases the gas power and hence increases the compressor speed deceleration during trip. Consequently, the safety system has less time to react and thereby the compressor is more prone to surging.

Valve performance

The concept of Cv, or valve flow coefficient, was developed years ago by valve manufacturers. The parameter is defined as the amount of water at 60 °F that will flow though the valve in one minute, when the differential pressure across the valve is one pound per square inch. Although this may not be a normal situation in practice, it provides a systematic basis regarding valve sizing. The general definition of the flow coefficient is given by Equation 15. It should be emphasized that this equation is only valid for single-phase flow.

$$C_v = Q\sqrt{\frac{SG}{\Delta p}} \tag{15}$$

The IEC 60534-2-1 valve standard [26] is primarily applied to single-phase flow, in the form of either liquid or gas. In the case of cavitation or flashing empirically developed correction factors are used to correct the flow rate. However, these standards are no longer applicable if two-phase flows are to be considered at the valve inlet, see Darby et al [27] and Schmidt [28]. Therefore, various methods are in use today, by both plant operators and manufacturers, for predicting the multiphase flow capacity of valves. Consequently, this leads to different and largely incomparable results.

Today, the *addition model* represents perhaps the most common valve prediction model for two-phase flow in the industry. It is praised for its simplicity, dealing with each phase separately using the equations in the IEC 60534-2-1 Standard. The single-phase gas and liquid flow coefficients are added as weighted averages, comprising the multiphase flow coefficient. The addition method equation is presented below.

$$C_{v,mp} = GVF\frac{Q}{417F_p pY}\sqrt{\frac{SG_g TZ}{\Delta p}} + (1 - GVF)\frac{Q}{0.865F_p}\sqrt{\frac{SG_l}{\Delta p}} \tag{16}$$

However, no heat, mass or momentum transfer is considered in this model. The same goes for boiling liquids and flashing. If either flashing or liquid boiling through the valve is considered likely, use of homogenous non-equilibrium models should be considered. The current work deals with a gas dominated air/water mixture at ambient conditions. Further, the valve differential pressure is low. Thus, the risk of flashing, cavitation or liquid boiling is considered minimal. For these reasons, the addition model was considered a valid approach with regard to valve performance studies.

3 DYNAMIC PROCESS SIMULATION

For dynamic simulation a mathematical model is necessary that describes the time-dependent behavior of a physical system, in this case a compressor and a process. Such a model consists of a set of differential and algebraic equations that are implemented in a simulation program. This chapter provides an introduction to dynamic process simulation, more specifically: The working principles of Hysys Dynamics.

3.1 Introduction to Hysys Dynamics

The Hysys Dynamics process simulator contains a fully rigorous plant simulation package, utilizing first principle thermodynamic, mechanical and chemical relationships. The mathematical modeling is based on conservation relationships for mass, components and energy. These equations are represented by ordinary differential equations (ODEs) and solved iteratively using the Implicit Euler Method. Hysys uses lumped models for all of the unit operations, e.g. pipes, valves, coolers. This means that all physical properties are considered to be equal in space. Only the time gradients are considered in the analysis.

Hysys can be run in both steady state and dynamic mode. Emphasis will be given to the dynamic working principles, since this mode has extensively been used in the current work.

Integration strategy

When running Hysys in dynamic mode, the equations for all unit operations are solved simultaneously. This enables the possibility of accumulation within the process equipment, which is a vital part of dynamic analysis. The governing equations are:

- Volume (pressure-flow)
- Energy
- Composition

Computing these relation for every time step would be computationally expensive. Hence, the compromise is to solve the balances at different time step frequencies. The default solution frequencies, which are multiples of the integration time step, are one, two, and ten for the pressure-flow equations, energy, and composition balances. Since composition tends to change much more gradually than the pressure, flow, or energy in a system, the equations associated with composition can be solved less frequently.

Holdup model and pressure-flow solver

Dynamic behavior arises because most plant equipment has some sort of material inventory or *holdup*. A holdup model is necessary because changes in the composition, temperature, pressure or flow in an inlet stream to a given process equipment are not immediately seen in the exit stream. The lagged response that is observed in any unit operation is the result of the *accumulation* of material, energy, or composition in the holdup.

The pressure-flow solver is one of the governing relations in Hysys Dynamics. Almost every unit operation in the simulation model can be considered a holdup or carrier of material (pressure) and energy. A network of pressure holdups can therefore be conceived across the entire simulation case. The pressure-flow solver considers the integration of pressure-flow balances within the simulation case. There are two basic equations which define most of the pressure-flow network:

- Resistance equations - Define flow between pressure holdups.
- Volume balance equations - Define the material balance at pressure holdups.

The pressure-flow balances both require information from and provide information to the holdup model. The holdup model calculates the accumulation of material, energy, and composition in the holdup, while the pressure-flow solver determines the pressure of the holdup and the related flow rates. Figure 7 illustrates the concept for a typical compressor system. For simplicity, the sum of process equipment between flow calculators (resistance equations) is defined as a “pressure holdup”.

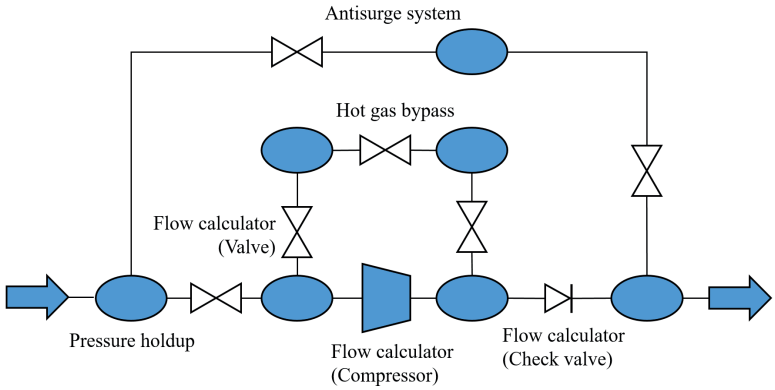

Figure 7: Simplified simulation network of a typical compressor system

Centrifugal compressor

To model the compressor performance characteristics accurately, the compressor block can employ several performance speed curves. If the compressor speed equals the speed of one of the specified performance curves, then only this performance curve is used. In the case where the compressor speed lies between two performance curves, a linear interpolation is performed. If the speed lies outside the performance envelope, a new performance curve will be calculated based on affinity laws of the closest available curve.

For a single-stage, low Mach number compressor (Ma < 0.3, incompressible fluid), the variation in head and capacity with speed tend to follow the affinity laws accurately. The deviation increases for multistage compressor systems operating at high pressure ratios. The volume flow rate is proportional to the rotational speed (Equation 17). The polytropic head varies proportionally to the square of the rotational speed (Equation 18). The power follows the cube of the rotational speed (Equation 19).

$$Q \propto \omega \rightarrow \frac{Q_A}{Q_B} = \frac{\omega_A}{\omega_B} \tag{17}$$

$$H \propto \omega^2 \rightarrow \frac{H_A}{H_B} = \left(\frac{\omega_A}{\omega_B}\right)^2 \tag{18}$$

$$P \propto \omega^3 \rightarrow \frac{P_A}{P_B} = \left(\frac{\omega_A}{\omega_B}\right)^3 \tag{19}$$

The compressor performance calculations support polytropic analysis, which is based on Schultz method. Naturally, the compressor performance results are dependent on the input conditions. If the inlet conditions, compressor speed and the performance curves are known/provided, Hysys first uses the curves to determine the polytropic head and efficiency, then calculates outlet pressure, temperature and applied duty.

4 EXPERIMENTAL RESULTS AND ANALYSIS

This chapter summarizes the experimental work, which form the foundation for model simulation and validation. The topics presented here include: Compressor hysteresis, compressor performance in wet gas flow and the impact of inlet slugging on compressor/system performance.

4.1 Compressor hysteresis

Previous studies performed at the test facility have reported the occurrence of compressor hysteresis at low inlet flow rates and high GMFs. Ferrara et al [29] detected marked compressor performance discrepancies at 0.92 – 0.88 GMF when gradually decreasing the flow rate towards surge. Hundseid et al [10] documented distinct compressor performance shifts when operating at 0.95 GMF at low flow rates, as shown in Figure 8.

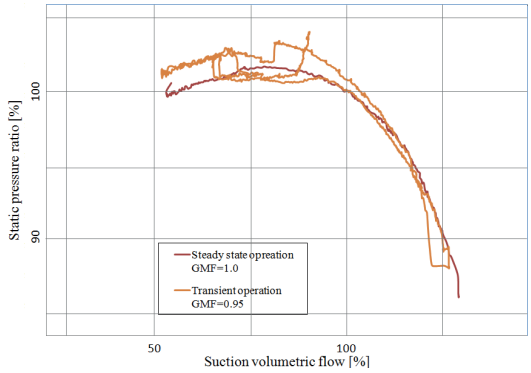

Figure 8: Compressor hysteresis at GMF 0.95 [10]

This behavior induces major challenges regarding compressor performance prediction and development of appropriate control logics to secure stable operation. In addition, it creates a complicated basis with respect to test and validation of dynamic simulation models. Hence, initial experimental studies were conducted to document and understand the onset of hysteresis. The test was carried out by gradually increasing the liquid content from a fixed gas flow rate (74% of design flow). Emphasis was put on compressor performance and its correlation to the diffuser multiphase flow characteristics. A video camera was utilized in the campaign, to capture both the diffuser section and the compressor operating point, as shown in Figure 9. Figure 10 shows the compressor performance characteristics and the test starting point.

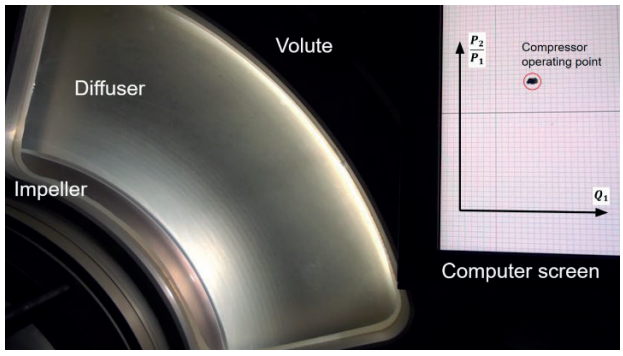

Figure 9: The diffuser section and a monitor capturing the compressor operating point

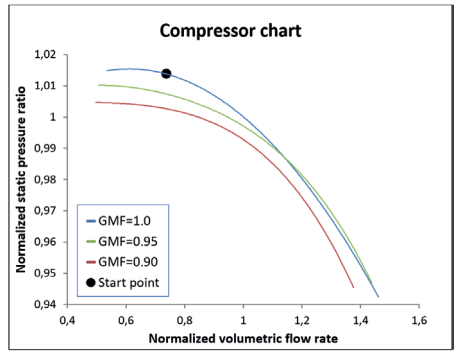

Figure 10: Compressor performance characteristics at 9000 rpm

GMF 1.0

The starting point of the test sequence is shown in Figure 11a. The dry operating point serves as a reference for the wet gas performance.

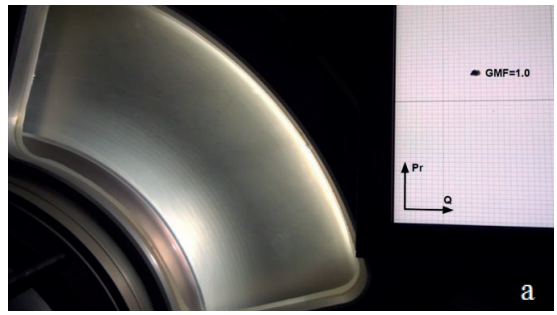

GMF 0.991

The initial liquid injection resulted in an increase of the compressor pressure ratio. The flow regime was characterized by tiny droplets dispersed in the gas phase. Limited deposition was detected on the diffuser hub and shroud side.

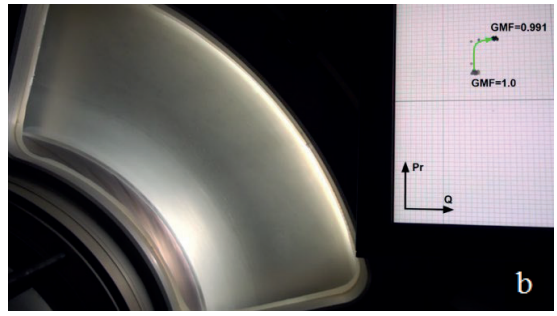

GMF 0.970

When decreasing the GMF to 0.970, liquid accumulation was detected on the hub side of the diffuser discharge, as highlighted in Figure 11c. A drop in both compressor pressure ratio and flow rate was documented.

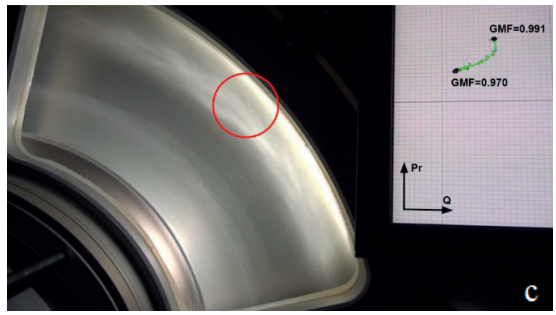

GMF 0.951

At 0.951 GMF a change of diffuser flow regime was detected, consisting of a uniform liquid film flow on the entire diffuser hub side. A small drop in static pressure ratio was detected in these conditions.

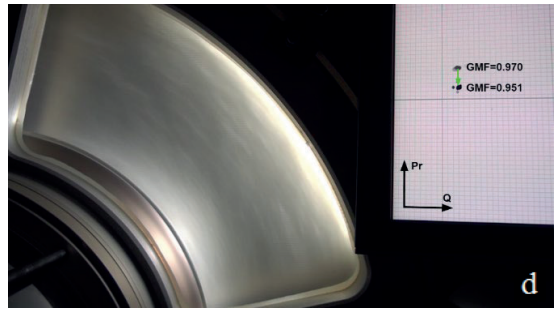

GMF 0.921

No change of diffuser flow regime was detected. A small drop in both pressure ratio and volume flow rate was documented.

GMF 0.907

Diffuser instability. A continuous shift of flow patterns was observed. Distinct performance fluctuations were detected, showing a clear dependence between the diffuser flow characteristics and the compressor performance. Surprisingly, the pressure ratio increases, which is in contrast to the compressor characteristics.

GMF 0.896

Decreasing the GMF to 0.896 caused the flow regime to change and stabilize. Liquid could clearly be seen accumulating in the diffuser discharge, similarly to Figure 11c, but this time on the diffuser shroud side. A marked drop in both compressor pressure ratio and volume flow rate was detected.

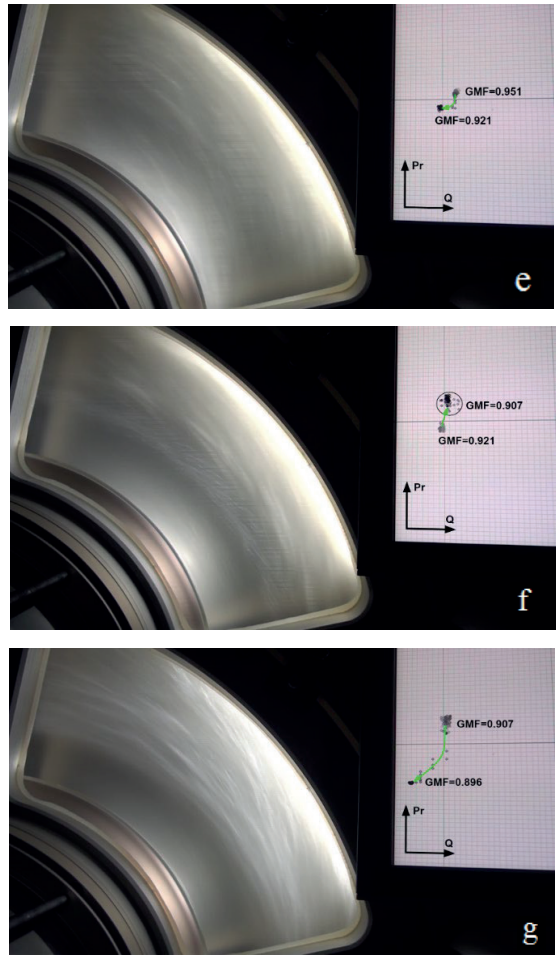

Figure 11: Compressor performance and diffuser flow regime at GMF a) 1.0 b) 0.901 c) 0.970 d) 0.951 e) 0.921 f) 0.907 g) 0.896

Figure 12 shows the entire compressor path, ranging from GMF 1.0 to GMF 0.896. The result is surprising because the operating point does not steadily decrease, as the compressor performance curves, when the liquid content increases. Furthermore, there are several operating points which stand out. Of these, the GMF 0.907 operating point stands out the most. The distinct performance deviation from the GMF 0.90 performance curve, marked pressure fluctuations, occurrence at low flow rates and complex three-dimensional flow suggests that the compressor was in hysteresis. Although the onset of this behavior is yet to be fully understood, it is worth mentioning that the flow regimes of the adjacent operating points are of fundamental difference. A continuous liquid film flow was detected on the diffuser *hub side* at GMF 0.921, whereas liquid accumulation on the diffuser *shroud side* was observed at GMF 0.896. Hence, the unsteady flow characteristics at GMF 0.907 may be an unsteady transition between these two flow regimes.

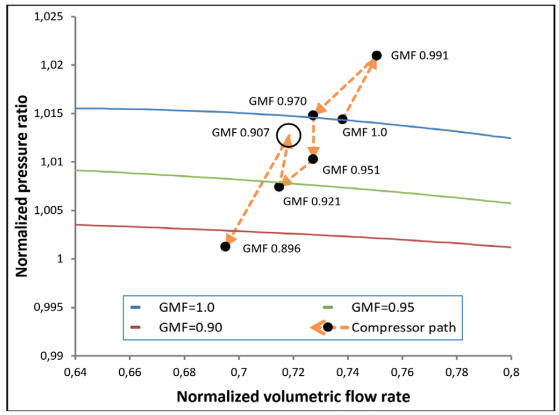

Figure 12: Compressor performance from GMF 1.0 to GMF 0.896

By investigating the diffuser flow regime at GMF 0.970 frame by frame, it appears that the accumulated liquid originates from the volute, as illustrated in Figure 13. The accumulated liquid stagnates in a fixed radial position in the diffuser owing to volute backflow outbalancing the mixture momentum from the impeller discharge. This flow phenomenon represents blockage, which impacts the diffuser pressure recovery. A distinct drop in both compressor pressure ratio and flow rate was detected at these conditions.

Figure 13: Diffuser flow transition from GMF 0.991 to GMF 0.970

Investigation of the diffuser flow regime at 0.951 is consistent with the observations above. Studying the pictures frame by frame when increasing the liquid content from GMF 0.970 to 0.951 reveals that the accumulated liquid accelerates radially inwards toward the impeller discharge, resulting in a uniform liquid film flow on the entire diffuser hub side. This is illustrated in Figure 14. This suggests that increasing the liquid content at the given flow rate amplifies the volute backflow, forcing the accumulated liquid inwards against the impeller discharge. This influences both the diffuser flow characteristics and the compressor performance.

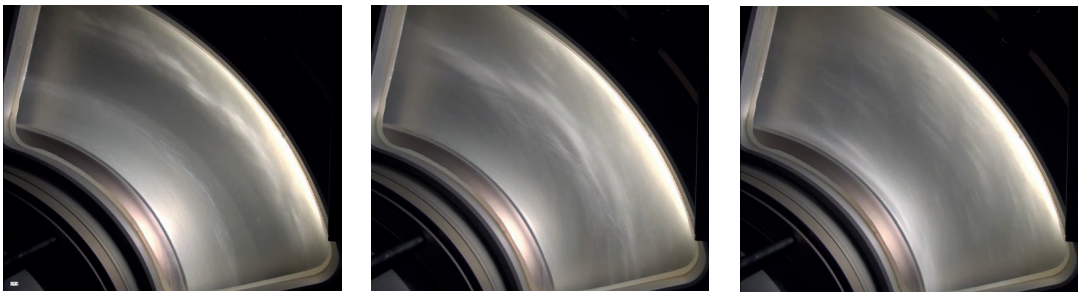

Figure 14: Diffuser flow transition from GMF 0.970 to GMF 0.951.

Further tests were conducted with the goal to illuminate how the diffuser/volute interaction influences the compressor performance characteristics. The compressor curves were established going from high to low flow rates. Emphasis was given to the diffuser/volute flow characteristics and their correlation to the compressor performance.

The investigation revealed that there was a link between the volute flow characteristics and the compressor performance. In monitoring the volute flow regime, it was observed that the high-density liquid behaves differently in comparison to dry gas diffusion in a circular volute. Rather than diffusing evenly, the liquid segregates and establishes a dominant flow direction. Consequently, at lower flow rates segregated liquid tends to swirl along the volute wall and re-enter the diffuser, hence "penetrating" the opposite diffuser exit boundary layer, as illustrated in Figure 15. This confirms the hypothesis that the observed liquid backflow in the diffuser originates from the volute. At high flow rates the liquid flow in the volute was consistently found to swirl from the diffuser *shroud to hub* side (SH). This was documented for all tested GMFs. However, at low flow rates a change of volute flow direction was detected, swirling from diffuser *hub to shroud* side instead (HS). Figure 16 shows two photographs of the liquid flow in the volute.

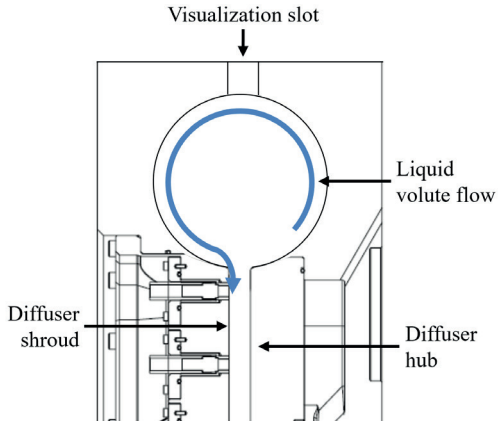

Figure 15: Liquid flow swirling from diffuser hub- to shroud

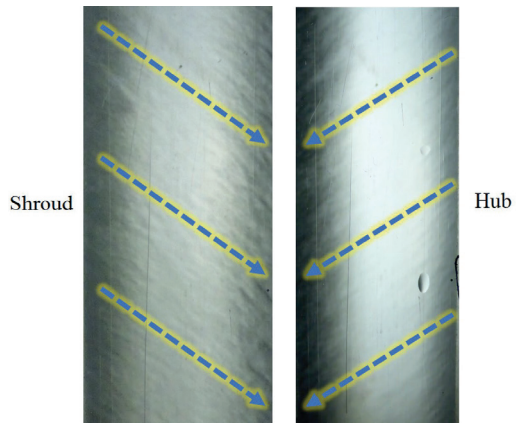

Figure 16: Observed volute flow direction. Left: Shroud to hub. Right: Hub to shroud

Figure 17 and 18 shows the compressor performance in context with the volute flow characteristics at GMF 0.975 and GMF 0.95. The *SH* flow regime was detected almost throughout the characteristics. The only exception was at 50% flow rate where the *HS* flow regime was observed. Both operating points show a small pressure ratio increase, although it is difficult to determine to what degree this is due to the diffuser/volute flow characteristics. When decreasing the flow rate additionally mild surge was detected. Consequently, the volute flow regime became too unstable to determine a dominant liquid flow direction.

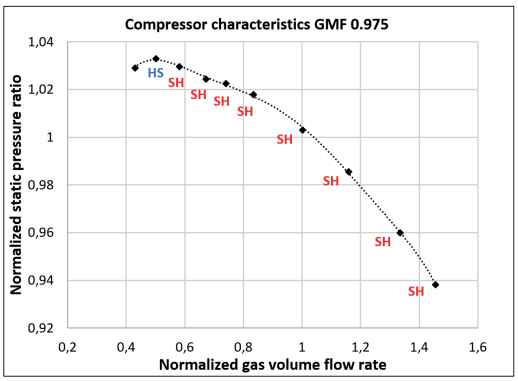

Figure 17: Compressor performance GMF 0.975

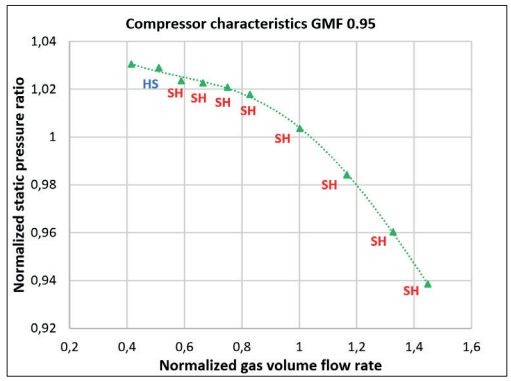

Figure 18: Compressor performance GMF 0.95

To illuminate the performance impact of the two flow characteristics, a second test was performed. The test was initiated at low flow rates with the *HS* flow characteristics. From here the flow rate was gradually increased while keeping the GMF constant. The volute flow characteristics was continuously monitored to document the onset of flow regime change. Table 3 shows the test start conditions.

Table 3: Test start conditions

	GMF	Gas volume flow rate	Volute flow regime	Stabilization time
Start point	0.99	75%	HS	60 sec
Start point	0.975	50%	HS	60 sec
Start point	0.95	50%	HS	60 sec

Figure 19 and 20 shows the performance impact of the two flow regimes at GMF 0.975 and GMF 0.95. The HS flow regime was documented from the test start point to a gas flow rate slightly above design flow, where the volute flow characteristics changed to SH. Simultaneously, a small pressure ratio drop was detected. From here, the gas volume flow rate was gradually decreased towards the starting point, resulting in a complete match with the original compressor characteristics.

The HS flow regime entailed a significantly higher compressor pressure ratio, in addition to increased polytropic efficiency. At GMF 0.95 at 75% flow rate a 2.6% (pp) efficiency increase was found relative to the SH flow regime. Furthermore, the shape of the curves, i.e. pressure rise, is markedly different, which influences compressor stability. It can also be seen that the onset of volute flow regime change gradually moves towards higher flow rates at reduced GMF. This suggests that increased liquid content increases the swirling liquid momentum in the volute, which makes the established flow characteristics less prone to disturbances.

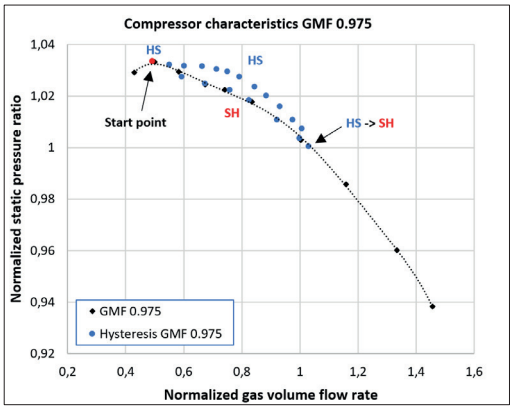

Figure 19: Diffuser/volute flow impact on compressor performance at GMF 0.975

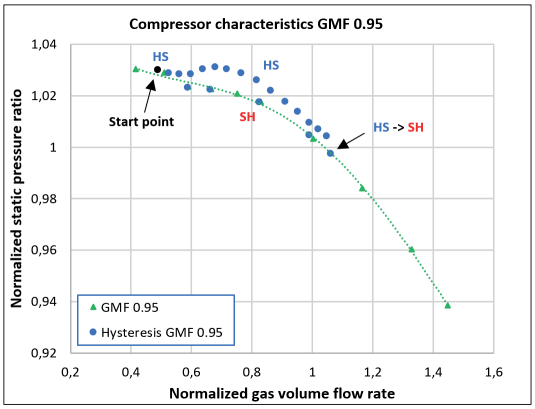

Figure 20: Diffuser/volute flow impact on compressor performance at GMF 0.95

Revised design - Diffuser trim

Compared to dry gas, wet gas entails a marked shift in thermodynamic and fluid properties for the entire stage. First of all, the discharge temperature is significantly lower owing to liquid heat capacity and evaporation. Second, wet gas entails an increased pressure ratio, i.e. increased discharge pressure at fixed inlet pressure. The combined effect is reduced diffuser velocities, which may result in a mismatch between the impeller and the diffuser. A reduced diffuser velocity will make the diffuser less resistant to liquid backflow from the volute. Hence, the diffuser thickness was reduced by 15% to investigate the impact on compressor performance. Figure 21 and 22 show the performance impact at GMF 0.975 and 0.95, going from high to low flow rates while monitoring the volute flow characteristics. It can be seen that the shape of the performance curves, i.e. pressure rise, is markedly different in comparison to the original diffuser setting. Still, a change in volute flow characteristics was present at low flow rates. To investigate the performance impact of the two flow characteristics with the current diffuser setting, the performance test (Table 3) was repeated. The test start was at low flow rates with the HS flow characteristics. The results reveal that the performance impact is negligible

although a change of volute flow characteristics is present. This implies that the segregated volute flow is not able to influence the diffuser flow characteristics and compressor performance in the same manner as documented above.

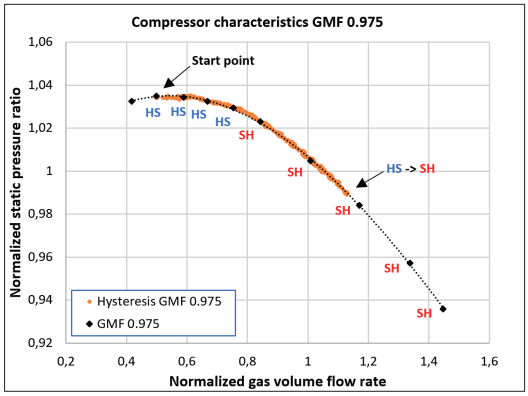

Figure 21: Compressor performance at GMF 0.975 – Revised diffuser design

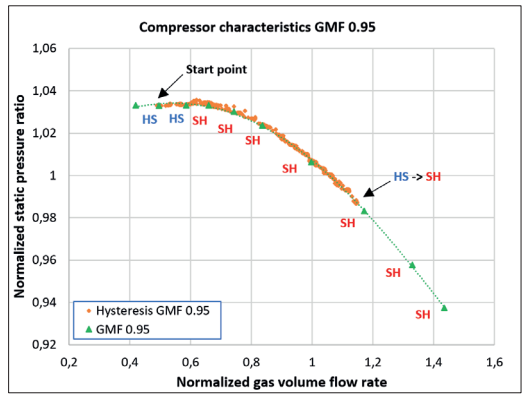

Figure 22: Compressor performance at GMF 0.95 – Revised diffuser design

Summary and conclusion

An experimental test campaign has been conducted on a centrifugal compressor to investigate compressor hysteresis. Initial tests revealed the occurrence of volute backflow at low flow rates. The backflow had clear impact on the diffuser flow characteristics and the compressor performance for the tested GMFs. Further tests confirmed the claim that the observed liquid backflow in the diffuser originated from the volute. In monitoring the volute flow characteristics, it was observed that the high density liquid behaves differently in comparison to dry gas diffusion in a circular volute. Rather than diffusing evenly, the liquid segregates and establishes a dominant flow direction. Consequently, at low flow rates segregated liquid tend to swirl along the volute wall and re-enter the diffuser, hence "penetrating" the opposite diffuser exit boundary layer. Depending on the volute flow direction (HS or SH) and its interaction with the diffuser, a distinct performance impact was documented. In addition, the shape of the curves, i.e. pressure rise, was affected by the flow characteristics, which in turn influences compressor stability. Narrowing the diffuser width by 15%, hence increasing diffuser velocities, improved the compressor performance. Although a change of volute flow characteristics was still present, the impact on the compressor performance was negligible.

It can be concluded that the interaction between the impeller, diffuser and volute is vital to understand with respect to wet gas compressor performance and stability. In addition, care should be taken when it comes to utilizing established dry gas compressor design on wet gas compressors, as the two phases behaves fundamentally differently through the compressor stage.

4.2 Wet gas compressor performance

Establishment of accurate and repeatable wet gas performance data is paramount, as it forms a necessary basis for model simulation. This section analyzes the compressor performance in wet gas flow. The compressor was exposed to liquid contents ranging from GMF 1.0 to 0.60. The compressor characteristics were established by going from high to low flow rates, utilizing the discharge throttle valve.

Figure 23 shows the compressor performance characteristics (static compressor pressure ratio vs total volumetric flow rate). It can be seen that wet gas entails a higher compressor pressure ratio around best efficiency point and at low flow rates. At maximum flow rate, the added liquid content shows a clear impact on the flow throughput. This is linked with increased droplet deposition rates and increased momentum transfer between the phases through the compressor and the following pipe system. Further, the wet gas performance curves coincide very well revealing that the pressure ratio varies little with respect to GMF.

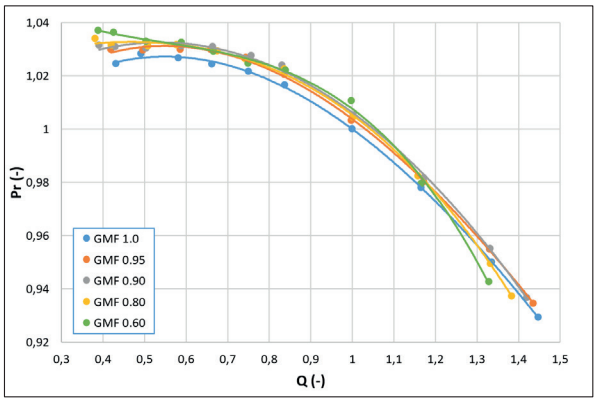

Figure 23: Compressor pressure ratio characteristics

The polytropic head characteristics form the basis for stability and anti-surge analyses. Several sources document the wet gas impact on surge point location, Ferrara et al [29] [30]. In conclusion, the fluid liquid content does not alter the surge point location towards higher inlet flow rate or ruin the surge stability margin. Figure 24 shows the polytropic head against the total volumetric flow rate. In contrast to the pressure ratio, the polytropic head decreases substantially when the liquid content is increased. This is linked with the significantly lower head requirement for the liquid phase, resulting in an overall head decrease. The "head rise to surge" is an important criterion for surge stability evaluation. From Figure 24 it is evident that increased liquid content results in a reduced "head rise to surge". Thus, with the standard requirement of a minimum head rise to surge (API 617), it *appears* that the compressor operating range is significantly reduced as liquid content increases.

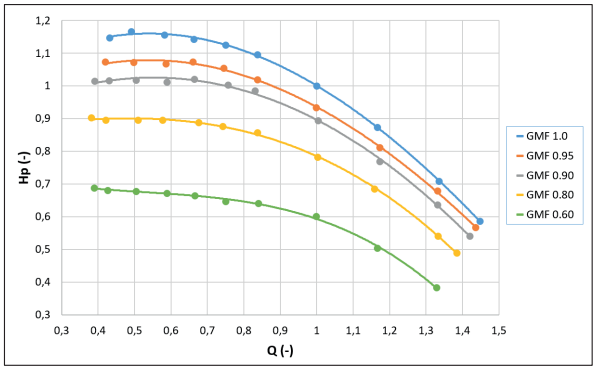

Figure 24: Polytropic head against total volumetric flow rate

However, the wet compressor control system reacts to measured process variables like the compressor pressure ratio. The pressure ratio characteristics do not vary significantly with respect to GMF, as shown in Figure 23. In summary, although the "head rise to surge" decreases as liquid content increases, the actual "pressure rise to surge" remains and gives a satisfactory stability margin. In this regard it is vital to utilize consistent and reliable wet thermo- and fluid dynamic property calculation to reproduce actual wet compressor pressure rise performance and predict the real plant behavior.

Figure 25 shows the polytropic efficiency against the total volumetric flow rate. Consistently with previous studies [11] [12], the polytropic head and efficiency decreases with increasing liquid content. At GMF 0.60 the efficiency curve reveals a peculiar trend. This must be analyzed in relation to the pressure ratio curve at GMF 0.60 (Figure 23), which shows a steady increase towards surge. Curves with similar shapes have previously been studied by the authors, Bakken et al [31], and found to occur in relation with volute backflow influencing the diffuser flow characteristics and performance, at low flow rates.

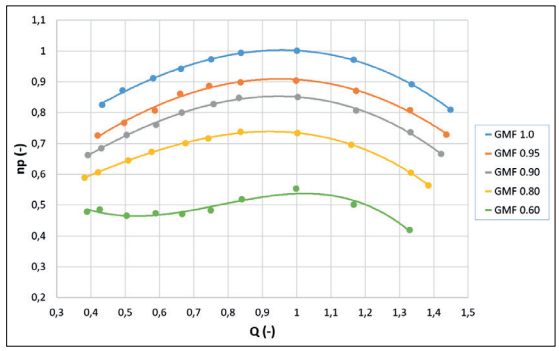

Figure 25: Polytropic efficiency against total volumetric flow rate

Summary and conclusion

Establishment of accurate and repeatable wet gas performance data is paramount, as it forms a necessary basis for model simulation. An experimental test campaign was conducted to analyze the compressor performance and stability in wet gas flow.

The test reveals that the pressure ratio increases and the polytropic efficiency decreases when introducing liquid. Care should be taken when analyzing stability and surge margins for different GMFs. Increased liquid content reduces both the polytropic head and "head rise to surge", while the "pressure rise to surge" remains, providing a satisfactory stability margin.

4.3 Inlet slugging on compressor performance

Inlet slugging represents a serious concern for wet gas compression systems, from both a mechanical and a performance perspective. The current section analyzes the compressor system behavior when subjected to inlet slugging. This forms a valuable basis with respect to model validation.

Inlet slugging was created in two different ways. In the first scenario, slugging was created artificially utilizing the liquid injection system. This is advantageous because one has full control of the inlet conditions, including the liquid flow rate, and the scenario is fully reproducible. In the second approach, liquid was collected in a negatively sloped inlet pipe 8.6 meters upstream of the compressor. By ramping the discharge valve open, hence increasing the pipe gas velocity substantially, a terrain slug was created. This represents a more realistic slug; however, control and repeatability are compromised. Figure 26 and 27 show the test arrangement. Table 4 and 5 show the test matrices for the two scenarios.

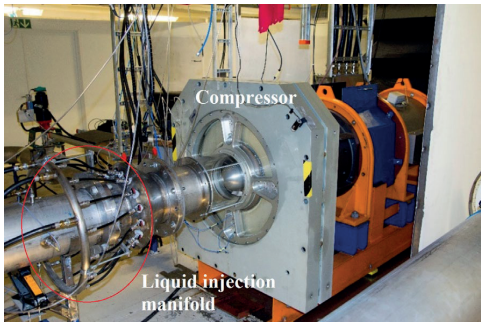

Figure 26: Test arrangement for artificial slug

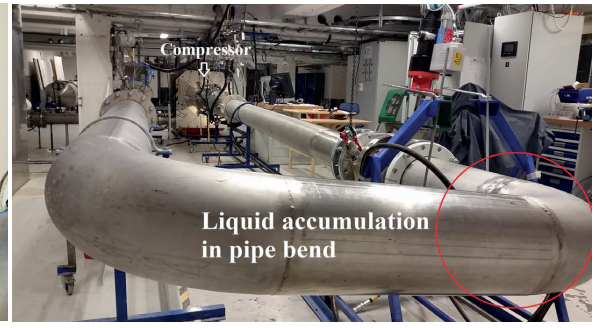

Figure 27: Test arrangement for terrain slug

Table 4: Test condition – Artificial slug

Artificial	Parameter	Quantity
	Compressor speed	9000 RPM
Slug trigger	Liquid valve	0% → 99%
	Gas flow rate*	1.55 (m^3/s)
	GMF / GVF	1.0 → 0.185 1.0 → 0.995

*Before slug initiation

Table 5: Test conditions – Terrain slug

Terrain	Parameter	Quantity
	Compressor speed	6000 RPM
Slug trigger	Discharge valve	40% → 99%
	Gas flow rate*	0.48 (m^3/s)
	GMF / GVF	1.0 → ?
	Pipe inclination	-2.1°

*Before slug initiation

Artificial slug

Figure 28 shows the initiation of the artificial slug. The liquid flow rate increases from 0 to 5.4 l/s in 600 milliseconds. A peak flow rate of 6 l/s was detected, which corresponds to a GMF of 0.185. Figure 29 shows the compressor speed and torque in correlation with the liquid flow rate. A massive torque increase was detected, ranging from 33 to 162 Nm, which equals an increase of 391% over 600 milliseconds. In the same time interval, the compressor speed drops from 8980 to 8770 rpm before the VSD starts recovering the speed.

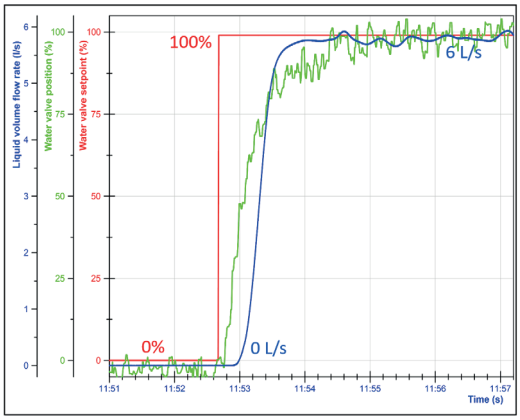

Figure 28: Artificial slug initiation – Water valve position and liquid flow rate

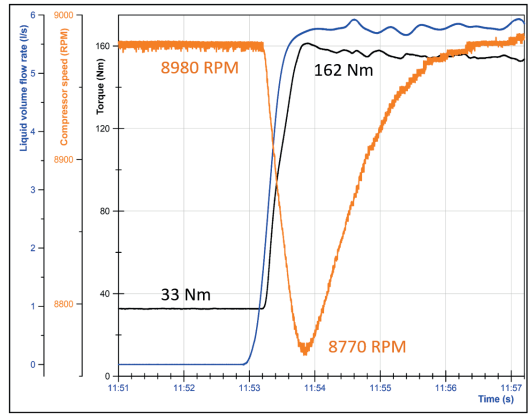

Figure 29: Artificial slug – Compressor speed and shaft torque

Figure 30 describes the gas volume flow rate and the compressor static pressure ratio. A distinct drop in the flow rate was found directly after slug initiation, which implies a marked throttling effect through the compressor and downstream pipe system. Simultaneously, an immediate drop in static pressure ratio is detected before it converges to 1.20. However, marked fluctuations can still be seen.

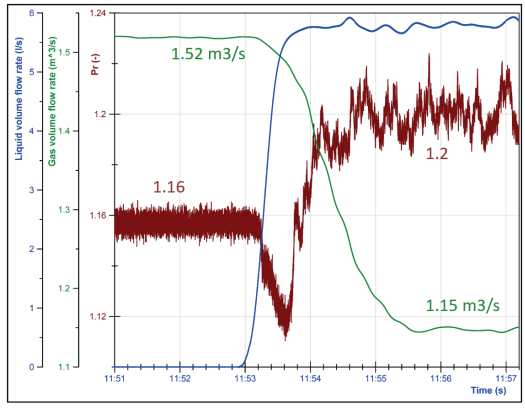

Figure 30: Artificial slug – Gas flow rate and static compressor pressure ratio

Terrain slug

Figure 31 shows the initiation of the terrain slug. An immediate increase in the gas volume flow rate can be seen following the discharge valve ramp-up. Thereafter a distinct drop is shown, suggesting that the liquid slug enters the compressor in this time interval. After the dip, the gas volume flow rate converges to 1.0 m^3/s.

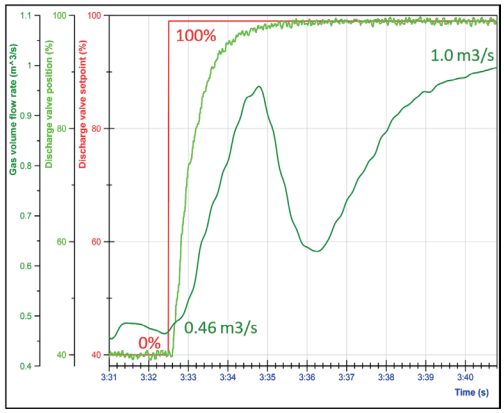

Figure 31: Terrain slug – Discharge valve position and gas volume flow rate

Investigating the compressor speed and torque enable more precise determination to when the liquid slug enters the compressor. The distinct drop in compressor speed, ranging from 5950 to 5730 rpm, and the marked shaft torque increase of 375% provide sound confirmation that the liquid bulk enters the compressor. Again, the gas flow rate decreases substantially. Figure 33 depicts the compressor static pressure ratio in context with the gas volume flow rate and the compressor speed. As the slug enters the compressor an immediate drop in static pressure ratio is seen. This result coincides with the behavior during the artificial slug, which confirms that this is the actual system behavior in the event of a slug.

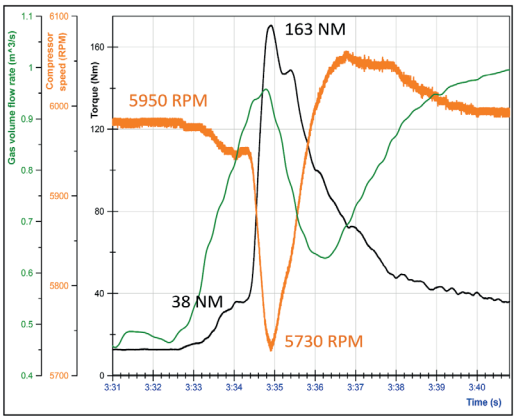

Figure 32: Terrain slug – Compressor speed and shaft torque

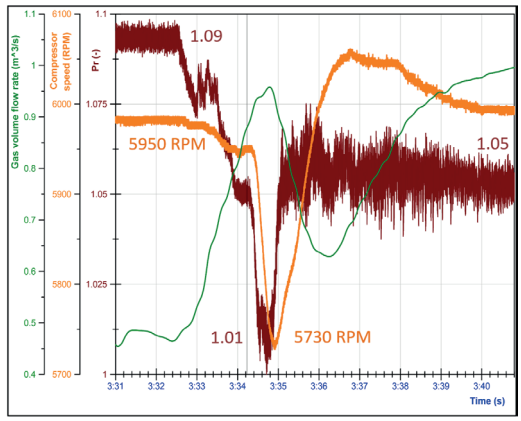

Figure 33: Terrain slug - Compressor speed and static compressor pressure ratio

Slugging in subsea wet gas compressor systems

Industrial compressor systems normally entail large inlet and discharge volumes, which will result in a slow pressure response in the case of transients. In addition, the available motor power is typically limited, to boost production. Hence, in the case of inlet slugging the fluid power increases substantially, which forces the compressor to decelerate (Equation 6). A slow pressure response forces the compressor to the left in the characteristics, towards surge.

Figure 34 illustrates the concept. The compressor is operating at design point at GMF 0.95. An inlet slug results in a speed drop and a new GMF of 0.70, shifting the operating point from point 1 to 2. Normally, the static compressor pressure ratio increases with increasing liquid content, which is beneficial with respect to compressor stability. However, some wet gas compressor concepts entail a lower static compressor pressure ratio at reduced GMF (Figure 35). This increases the transient response of the compressor system and has a greater impact on the capacity during slugging. Extra care should therefore be taken when integrating such wet gas compressor concepts into subsea boosting systems.

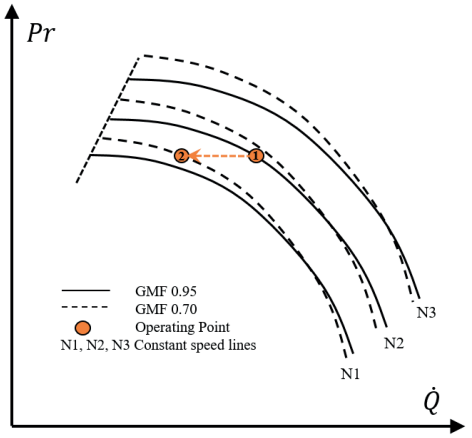

Figure 34: Compressor system response during inlet slugging – Increased performance at reduced GMF

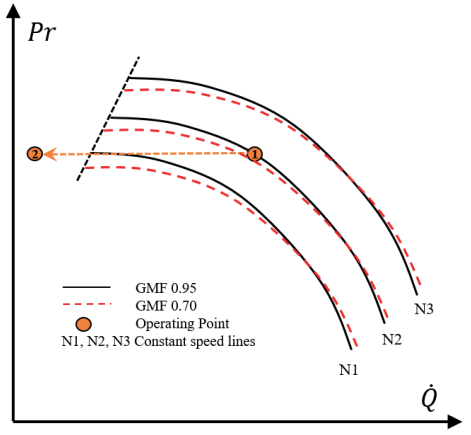

Figure 35: Compressor system response during inlet slugging – Reduced performance at reduced GMF

Summary and conclusion

Subsea compressor systems may suffer from large variations in GMF that may arise during start-up or when entering tail production of an oil and gas field. It is vital to understand the slug impact on the compressor and the related process and control system.

Two inlet slugging scenarios have been investigated and analyzed. The compressor performance and the drive show similar behavior regardless of scenario. The test revealed that the compressor is capable of handling multiphase flows as low as 0.185 GMF during inlet slugging, which in turn imposed a marked impact on the gas flow rate, compressor shaft torque and compressor pressure ratio. Inlet slugging may impose challenges for subsea compressor systems owing to the slow pressure response and the limited available power, which forces the compressor to the left in the characteristics, towards surge. The current work forms a valuable basis for model simulation and validation.

5 SIMULATION RESULTS AND ANALYSIS

This chapter presents the NTNU dynamic simulation model and aims to validate the working principles of the simulated wet gas compressor. Furthermore, the simulation model is be validated against transient test cases. Last, a driver trip case study from an export compressor system will be presented. The results form a basis for development of a concept called *digital compressor*.

5.1 Wet gas compressor modeling

In cooperation with Aspentech R&D, Hysys Dynamics has been extended to support modeling of wet gas compressors. This enables the user to input multiple performance curves at different GMFs as well as different compressor speeds. In addition, the user has the possibility to input multiple surge and stonewall curves based on the GMF. The candidate's contribution entails:

- Build and tune a dynamic model of the NTNU test facility
- Plan and perform experimental tests (both steady state and transient)
- Validate the functionality and accuracy of the wet gas compressor block against experimental data
  - Is linear interpolation between GMF performance curves an accurate approach?
  - Can the affinity laws be used to extrapolate performance curves in wet gas flow?
  - Validate the simulated compressor/system response against transient experimental data
- Contributions/advice regarding wet gas performance analysis and dimensionless parameters

When operating with multiple GMF performance curves in Hysys Dynamics there are two scenarios. Either the GMF at the compressor inlet equals the GMF of one of the performance curves, in which case the simulation model uses this performance curve only. If the GMF at the compressor inlet does not equal any of the provided performance curves, a linear interpolation is performed vertically along the GMF dimension between the two GMF curves closest to the current condition.

Interpolation along the speed dimension is similar to that along the GMF dimension when the current speed is within the limits of the input curves. When the speed is outside those limits, the *affinity laws* are used to estimate the compressor performance. This has proven to be a reasonable estimation for conventional dry gas compressor applications, however it remains to be validated whether the approach is applicable in wet gas flow. The compressor thermodynamic calculation method used in Hysys honors the *total fluid approach*, described in the introduction.

The accuracy of the compressor performance methodology when operating with multiple wet performance curves (linear interpolation method) has been validated against both air/water and hydrocarbon data. The applicability of the affinity laws in wet conditions has been validated against experimental data from the NTNU test facility.

NTNU dynamic simulation model

A dynamic simulation model has been built and tuned to replicate the wet gas compressor test facility at NTNU. The model can be used in various operating scenarios, i.e. both dynamic and steady state. Further, all relevant mechanical and process data are included. This comprises pipe lengths, bends, control valves, flow meter, liquid injection, and compressor data, including experimental performance curves. Both the GMF and the compressor flow rate can be controlled using proportional-integral-derivative (PID) controllers. Since the test facility is an open loop configuration, the ambient pressure serves as the boundary condition for both the inlet and discharge streams. The model is shown in Figure 36 highlighting the main process equipment.

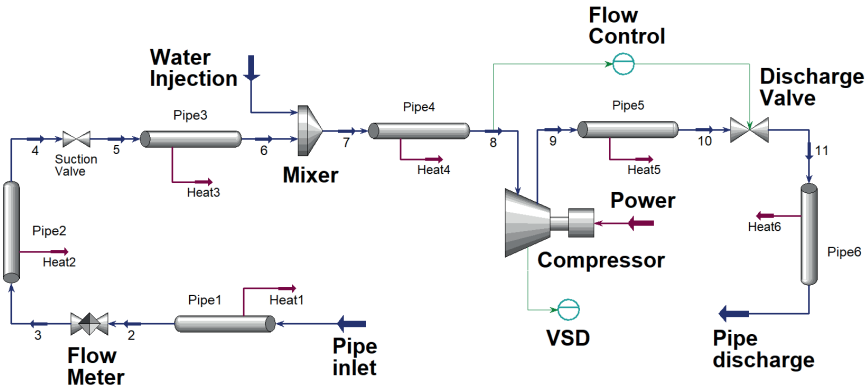

Figure 36: Dynamic simulation model of the NTNU test facility

The drive behavior has also been captured in the model utilizing a PID controller. This controller has two functionalities. First of all, one can set an upper torque threshold, limiting the available torque from the drive and hence the system response in transient test cases. Second, the drive controller has been tuned against experimental data to provide a similar response to transients. Figure 37 and 38 show the drive response when the compressor is subjected to a sudden increase of liquid content (inlet slug).

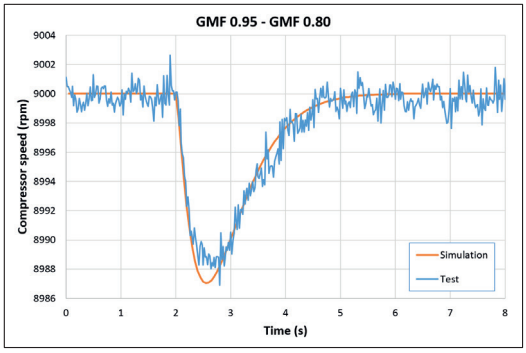

Figure 37: Sudden increase of liquid content and its impact on compressor speed

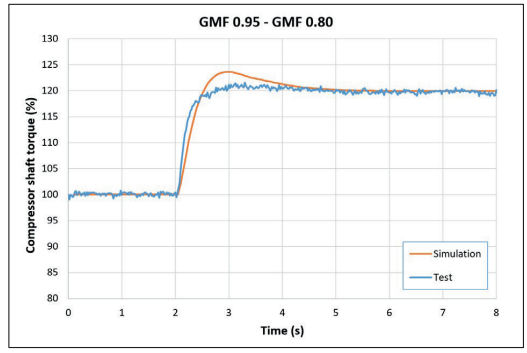

Figure 38: Sudden increase of liquid content and its impact on compressor shaft torque

5.2 Compressor performance methodology and model accuracy

The polytropic head and efficiency curves form the compressor performance basis in Hysys Dynamics, see Figure 24 and 25. The current section investigates the accuracy of the compressor interpolation procedure within the simulation model. Three different flow rates and two different GMFs were tested, making a total of six compressor operating points. The model was run until steady state conditions were achieved. Further, the model was set up in two different ways:

1) Use all GMF performance curves.
2) Force the model to interpolate by removing the GMF performance curve the model is operating at.

The second setup involves interpolation between the adjacent GMF curves. At GMF 0.95 this implies interpolation between the GMF 1.0 and GMF 0.90 curve. At GMF 0.90, the GMF 0.95 and GMF 0.80 curves were used for interpolation. Table 6 and 7 shows the results at GMF 0.95 and GMF 0.90 respectively. The performance data are plotted in % deviation of the experimental results, using equation 20.

$$\text{Deviation} = \left[\frac{\text{Simulation result}}{\text{Experimental result}} - 1\right] * 100 \quad (20)$$

Table 6 reveals a close correspondence between test results and simulation. When using all performance curves, the deviation in terms of polytropic head and efficiency becomes zero, whereas a negligible deviation can be seen for the compressor shaft power and static compressor pressure ratio. Although the deviation is slightly higher when interpolating, the results are still accurate, revealing less than 2.5 % maximum deviation. The deviation in inlet pressure remains approximately constant for the two model setups. This is expected since the flow rate (which is constant) dictates the pressure losses upstream of the compressor e.g. piping, orifice plate, and inlet valve.

Table 7 shows the interpolation accuracy of GMF 0.90. The overall accuracy is slightly reduced relative to the findings at GMF 0.95. This is to some degree expected, since the distance to the adjacent GMF curves is larger. It can be seen that the deviation in pressure ratio follows the deviation in polytropic head. The same goes for the compressor power, which is a function of the Hp and np (Equation 14).

Table 6: Simulation vs test at GMF 0.95

	Inlet conditions			% Deviation against performance data					
GMF = 0.95	Qinlet	GMF	Rh	Pin	Pr	Tout	Power	Hp	np
Using curves	1,33	0,95	61,2	-1,04	0,03	-0,13	0,12	0,00	0,00
Interpolation	1,33	0,95	61,2	-1,03	-0,08	-0,17	-1,60	-0,85	0,90
Using curves	1,00	0,95	61,4	-0,61	0,02	-0,09	0,38	0,00	0,00
Interpolation	1,00	0,95	61,4	-0,62	0,23	-0,11	-0,97	1,10	2,48
Using curves	0,75	0,95	59,6	-0,45	0,04	-0,05	0,68	0,00	0,00
Interpolation	0,75	0,95	59,6	-0,45	0,02	-0,09	-0,79	-0,14	1,35

Table 7: Simulation vs test at GMF 0.90

	Inlet conditions			% Deviation against performance data					
GMF = 0.90	Qinlet	GMF	Rh	Pin	Pr	Tout	Power	Hp	np
Using curves	1,33	0,90	49,5	-1,11	-0,01	-0,09	0,33	0,00	0,00
Interpolation	1,33	0,90	49,5	-1,12	-0,19	-0,13	-1,37	-1,33	0,37
Using curves	1,00	0,90	78,5	-0,61	-0,05	0,70	-0,61	0,00	0,00
Interpolation	1,00	0,90	78,5	-0,61	-0,52	0,64	-2,63	-2,59	-0,56
Using curves	0,75	0,90	76,9	-0,47	-0,04	0,72	-0,38	0,00	0,00
Interpolation	0,75	0,90	76,9	-0,47	-0,66	0,61	-4,06	-3,06	0,68

Validation against hydrocarbon data

The new compressor block was also tested against hydrocarbon data to ensure that the functionality and accuracy were applicable to different fluids and operating conditions. Performance data from a multistage centrifugal compressor operating in hydrocarbon flow served as foundation for the validation work.

Figure 39 and 40 describe the compressor performance. Inlet pressure and temperature were in the range of 25-30 bar and 285-295 K respectively. The polytropic head and efficiency decreases steadily as the liquid content increases. This is similar to the air/water data presented in Figure 24 and 25.

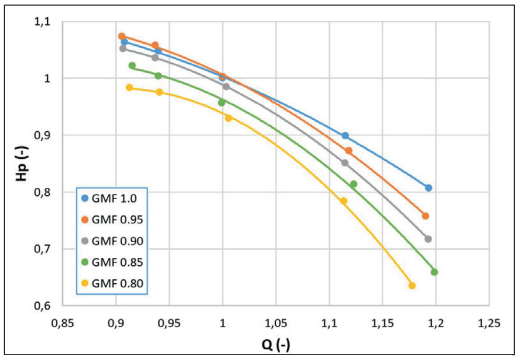

Figure 39: Polytropic head vs total volume flow rate for a multistage compressor operating in hydrocarbon flow.

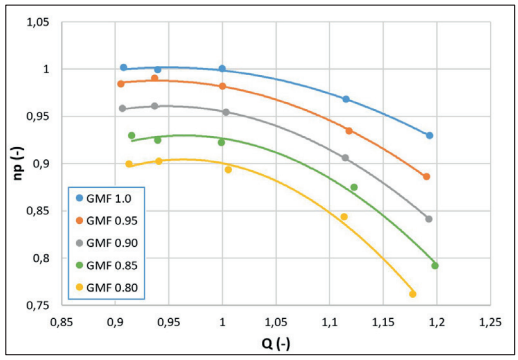

Figure 40: Polytropic efficiency vs total volume flow rate for a multistage compressor operating in hydrocarbon flow.

A dynamic model was created, with emphasis on the compressor itself and the correct inlet conditions e.g. composition, pressure, temperature, flow rate and GMF. To secure the correct composition and GMF upstream the compressor, the following inlet streams were mixed at the given pressure and temperature:

- Hydrocarbon liquids
- Hydrocarbon gases
- Water and MEG

A similar campaign was conducted as described in the previous section, with the intention of validating the accuracy of the compressor interpolation procedure in hydrocarbon flow. The polytropic head and efficiency curves, described in Figure 39 and 40, form the compressor performance basis within the model. Two GMFs, 0.95 and 0.85, were tested at three different flow rates, making a total of six operating points within the compressor envelope. The accuracy was tested both when using the performance curves and when interpolating between the adjacent GMF performance curves.

Table 8 shows the performance accuracy at GMF 0.95. Using all performance curves results in zero deviation in terms of polytropic head and efficiency. A small deviation can be seen for the compressor shaft power, pressure ratio and discharge temperature. Interpolation between a dry gas curve (GMF 1.0) and a wet gas curve (GMF 0.90) provides no difficulties for the model. The deviation remains below 1.5 %, which is considered accurate. Again, the pressure ratio follows the deviation in polytropic head, whereas the power follows the deviation in Hp and np. Similar observations can be made at GMF 0.85 (Table 9). Here too, interpolation results in a deviation of less than 1.5% in terms of polytropic head and efficiency.

Table 8: Simulation vs hydrocarbon performance data at GMF 0.95

	Inlet conditions		% Deviation of performance data				
GMF 0.95	GMF	Qinlet	Pr	Tout	Power	Hp	np
Using curves	0,95	0,94	0,85	-0,02	-0,17	0,00	0,00
Interpolation	0,95	0,94	-0,70	-0,16	-0,53	-1,45	-1,06
Using curves	0,95	1,00	0,84	0,00	0,52	0,00	0,00
Interpolation	0,95	1,00	-0,03	-0,11	0,11	-0,87	-0,42
Using curves	0,95	1,12	1,05	0,06	1,09	0,00	0,00
Interpolation	0,95	1,12	1,09	0,06	1,07	0,05	0,07

Table 9: Simulation vs hydrocarbon performance data at GMF 0.85

	Inlet conditions		% Deviation of performance data				
GMF 0.85	GMF	Q (-)	Pr	Tout	Power	Hp	np
Using curves	0,85	0,94	1,18	0,47	1,43	0,00	0,01
Interpolation	0,85	0,94	0,29	0,14	-0,11	-0,96	0,74
Using curves	0,85	1,00	1,23	0,46	1,36	0,00	0,00
Interpolation	0,85	1,00	1,44	0,44	1,19	0,16	0,34
Using curves	0,85	1,12	1,21	0,45	1,63	0,00	0,00
Interpolation	0,85	1,12	-0,03	0,32	1,16	-1,31	-0,82

Apart from the GMF, the fluid density ratio stands out as one of the most important fundamental parameters describing wet gas flow. Furthermore, the parameter incorporates both the inlet pressure and molecular weight, which are of great relevance. Figure 41 shows how the fluid density ratio influences the performance of the multistage compressor. The fluid density ratio is normalized against a composition consisting of only hydrocarbon gases and liquids. The parameter is reduced by replacing the hydrocarbon liquids with water. The plot shows clearly that the compressor performance, i.e. polytropic head, decreases as the fluid density ratio decreases. Heavier liquids separate more easily from the gas phase, while heavier droplets tend to deviate more from the gas flow lines. Consequently, heavier liquids account for increased droplet deposition, more slip between the phases and increased losses.

Figure 41 illuminates that the gas and liquid properties, and not only the GMF, provide vital information with respect to compressor performance in wet gas flow. This shows that dimensionless parameters describing the liquid properties relative to the gas properties, e.g. the fluid density ratio, need to be accounted for and incorporated into wet gas compressor simulation applications.

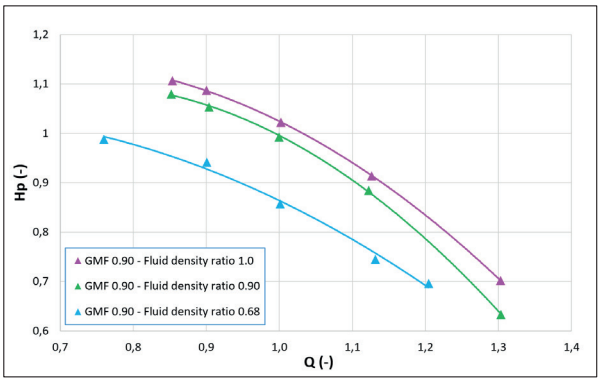

Figure 41: The fluid density ratio impact on the performance of a multistage centrifugal compressor in hydrocarbon flow.

Applicability of the affinity laws in wet gas flow

The affinity laws have been used extensively by the industry and within process simulation tools, such as Hysys Dynamics, for performance scaling and estimation. The current section evaluates the accuracy of the affinity laws against experimental wet gas performance data, performed at the NTNU test facility. The compressor speed was increased stepwise from 9000 rpm to 11000 rpm. Three different flow rates and three different GMFs were subject to investigation.

Figure 42 shows the compressor performance scaling when subjected to a stepwise increase of rotational speed. The results reveal that the compressor scales in a similar manner regardless of GMF. That is, the slope (dPr/dQ) is hardly affected by the GMF and the relative position between the dry and wet operating points remains close to constant as the speed increases. A similar observation can be made for the polytropic head, shown in Figure 43.

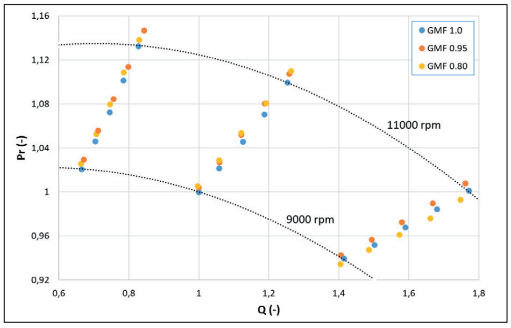

Figure 42: Compressor performance scaling in terms of static compressor pressure ratio and total volume flow rate.

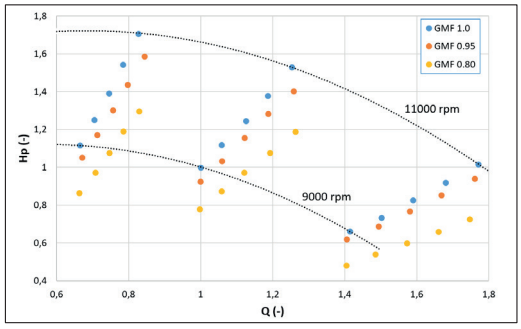

Figure 43: Compressor performance scaling in terms of polytropic head and total volume flow rate.

A prerequisite for utilizing the fan laws is that the compressor efficiency remains constant. Figure 44 shows that the polytropic efficiency is close to constant at high flow rates. However, at best efficiency point (BEP) and low flow rates the efficiency increases slightly. The biggest increase was documented at GMF 1.0 at low flow rates, revealing a 2.5% efficiency differential from 9000 to 11000 rpm. Although the efficiency is slightly increasing at BEP and low flow rates, the trend is similar for dry and wet gas. This suggests that the accuracy of the affinity laws should be of the same magnitude, in terms of polytropic head and power consumption, for the tested GMFs.

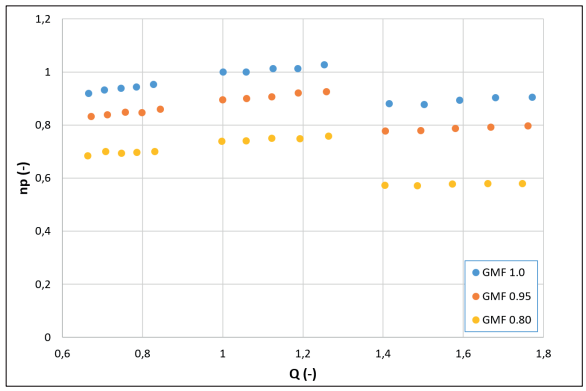

Figure 44: Compressor performance scaling in terms of polytropic efficiency and total volume flow rate.

Figure 45 shows the compressor performance scaling in relation to the affinity laws. In general, the affinity laws match the experimental results well for all tested GMFs. No major difference can be detected regarding the accuracy of the affinity laws for dry gas versus wet gas. In fact, the affinity laws match the wet gas operating points slightly better, in terms of polytropic head. When it comes to the flow rate, no general conclusion can be made. At BEP wet gas deviates more than dry gas; however, at high flow rates the exact opposite is the case. Table 10 shows the deviation between the test and the affinity laws at BEP. The deviation remains below 4%.

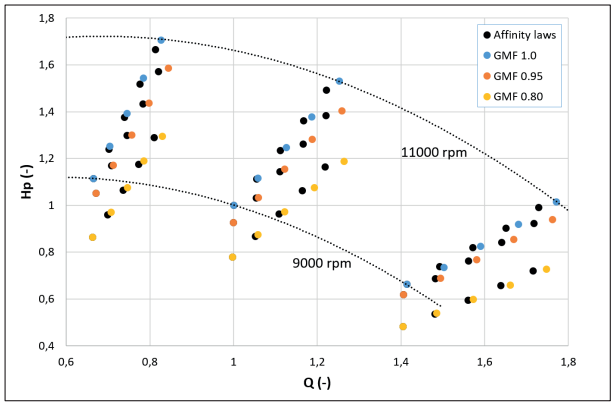

Figure 45: Tested compressor performance in comparison to the affinity laws.

Table 10: Deviation between compressor performance and the affinity laws at BEP.

BEP	GMF 1.0			GMF 0.95			GMF 0.80		
Speed (rpm)	Q (%)	Hp (%)	Pshaft (%)	Q (%)	Hp (%)	Pshaft (%)	Q (%)	Hp (%)	Pshaft (%)
9000	0,0	0,0	0	0,0	0,0	0	0,0	0,0	0
9500	-0,3	-0,4	-0,2	-0,5	-0,3	0,1	-0,6	-0,8	-0,7
10000	-1,3	-1,0	0,3	-1,0	-1,0	0,4	-1,2	-0,9	0,2
10500	-1,6	-1,2	0,2	-1,8	-1,6	1	-2,4	-1,3	-0,9
11000	-2,5	-2,5	0,2	-3,0	-1,5	1,1	-3,6	-2,0	-0,7

Summary and conclusion

In cooperation with Aspentech R&D, Hysys Dynamics has been extended to support modeling of wet gas compressors. This enables the user to input multiple performance curves at different GMFs as well as different compressor speeds. In addition, the user has the possibility to input multiple surge and stonewall curves based

on the GMF. Further, the affinity laws have extensively been used by the industry and within process simulation tools such as Hysys Dynamics for performance scaling. Experimental performance data have been used to validate the applicability of the affinity laws in wet gas flow.

The linear interpolation procedure within Hysys Dynamics has proved to be an applicable and accurate methodology. The results have been validated against both hydrocarbon and air/water performance data, within a GMF range of 1.0 to 0.8. The deviation between test and simulation in terms of polytropic head and efficiency was found to be less than 3.5 %. Striking similarities have been documented regarding compressor performance scaling in wet gas versus dry gas flow. The results reveal that the compressor scales in a similar manner regardless of GMF. That is, the slope (dPr/dQ) is hardly affected by the GMF and the relative position between the dry and wet operating points remain close to constant as the speed increases. The affinity laws match the experimental results well for all tested GMFs. No major difference can be detected regarding the accuracy of the affinity laws on dry gas versus wet gas. Thus, the affinity laws have proven to be applicable to wet gas flow for the current application.

5.3 Wet gas compressor model validation

The current section is divided into three. The first two sections present transient experimental performance data including comparison against model simulation. The last section is an experimental study on the discharge valve performance in wet gas flow.

Driver trip test

Trip of electrical drives represents a major threat for compressor systems owing to the instantaneous loss of driver power. Depending on several factors, e.g. the compressor characteristics and the safety system, the compressor may enter the surge region of the operating characteristics during run-down, causing high mechanical load and vibrations. Driver trip is also a serious concern for wet gas compression systems, which operate with a higher total mass flow rate and hence a higher fluid power.

A driver trip test was conducted to study the compressor behavior in dry gas vs wet gas flow. The power was cut from 100% to 0% within 10 ms, forcing the compressor to decelerate against the fluid power and friction losses; see Equation 6. The experimental results are shown in Figure 46 and 47. As expected, the compressor decelerates faster when more liquid is introduced. One second after trip initiation, the GMF 0.80 case shows a 30% larger speed drop relative to the dry gas case. This is critical for subsea/industrial compressor systems desiring a slow speed deceleration during trip, thereby giving the compressor safety system sufficient time to act. Hence, a faster speed drop may result in severe surging (Greitzer [32]) and mechanical failure, if no precautions are taken when operating in wet gas flow.

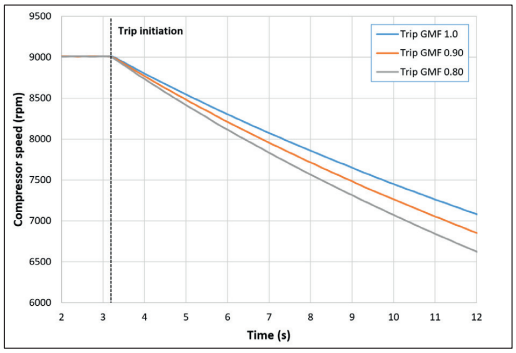

Figure 46: GMF impact on compressor deceleration

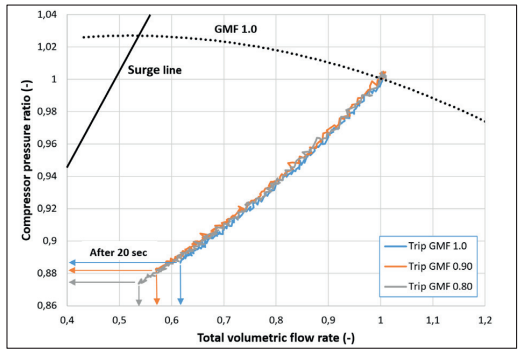

Figure 47: GMF impact on compressor performance during trip

Figure 48 shows the compressor speed deceleration during rundown against the simulation results. A very close agreement was found between the test and simulation in dry conditions. A satisfactory match is documented in wet conditions as well, revealing a maximum speed deviation of 3.2%, ten seconds after driver trip. The influence on the compressor pressure ratio is shown in Figure 49. Naturally, the model does not capture the fluctuations of the measured process variables. Regardless, a close correspondence can be seen between test and simulation.

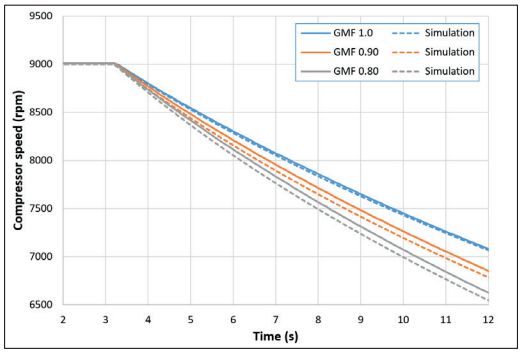

Figure 48: Compressor speed deceleration – Test vs simulation

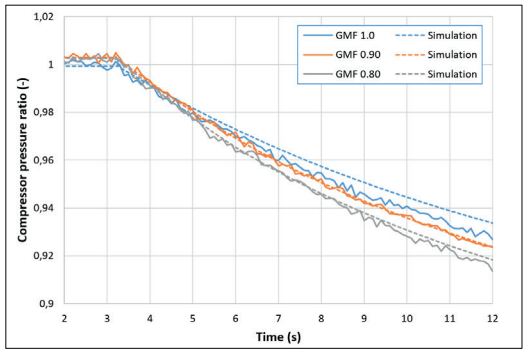

Figure 49: Static compressor pressure ratio – Test vs simulation

Gradual increase of liquid content

The following section analyzes how the compressor operating point moves within the performance characteristics when subjected to a stepwise increase of liquid content. The test was initiated from three different starting points on the GMF 0.95 performance curve: Low flow rate (triangle), best efficiency point (diamond) and high flow rate (square). The endpoints were at GMF 0.70, between the GMF 0.80 and GMF 0.60 performance curve. Although the test was conducted in a semi-transient manner, with only a brief hold time per operating point (60 sec), the experimental results match the compressor performance curves accurately. A greater impact on the flow rate was found when starting from high flow rates, whereas a more vertical trend can be seen at low flow rates. After all, more liquid is necessary to maintain a constant GMF at high flow rates.

The test was reconstructed in the simulation model, as shown in red. A satisfactory match was found between the test and simulation at low flow rate and BEP. At high flow rate, an increasing flow rate deviation was detected. This implies that there are higher flow restrictions in the system than the model accounts for. Further investigation was undertaken, with attention to the downstream control valve. Since the discharge valve characteristics implemented in the model is based on on-site dry gas tests, attention was given to the valve characteristics and it's applicability in wet gas flow.

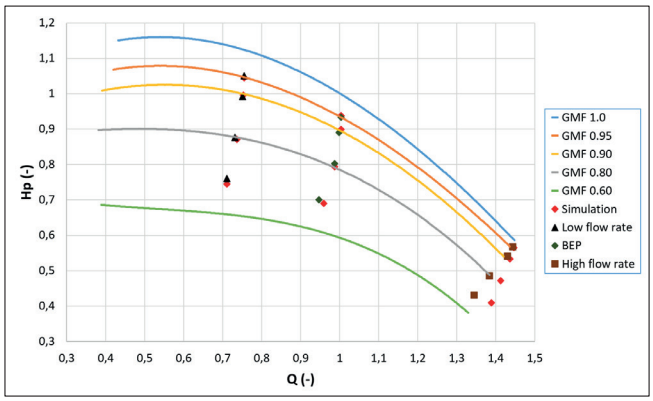

Figure 50: A stepwise increase of liquid content – Test vs simulation.

Multiphase valve performance

Experimental valve performance tests were performed to gain better insight into the valve behavior when subjected to wet gas flow. Figure 51 shows the total volumetric flow rate through the valve, revealing a flow rate decrease with increasing liquid content. The introduction of liquid creates a liquid boundary layer in the valve opening thereby decreasing the effective flow area resulting in increased throttling. Another factor influencing the flow throughput is droplet deposition. Droplets dispersed in the gas flow will not be able to follow the flow lines perfectly. Consequently, droplets will collide and deposit on the valve, form new droplets, and eventually reaccelerate when rejoining the flow. This creates a continuous momentum transfer between deposited droplets and the gas phase.

It can also be seen that the impact on the flow rate increases with increasing valve opening. This result was anticipated for two reasons. First of all, when operating at high gas flow rates, higher liquid flow rates are necessary to keep the GMF constant. Second, higher flow rates imply higher pipe velocities, which results in increased slip between the phases. The impact on the valve differential pressure is shown in Figure 52. The introduction of liquid increases the valve differential pressure. Again, this is connected with the increased throttling effect owing to liquid film flow though the valve. The most pronounced increase in differential pressure was found at GMF 0.80 at 100% valve opening, as indicated on the figure. A 49.1% increase was found here relative to dry conditions.

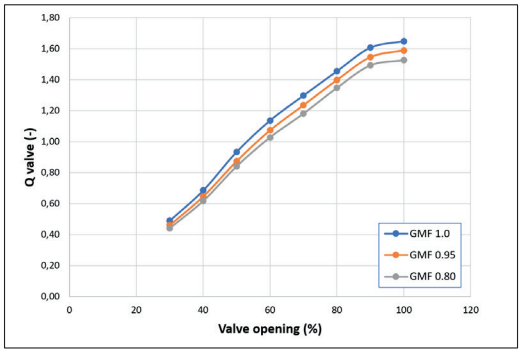

Figure 51: Valve inlet flow rate against valve opening

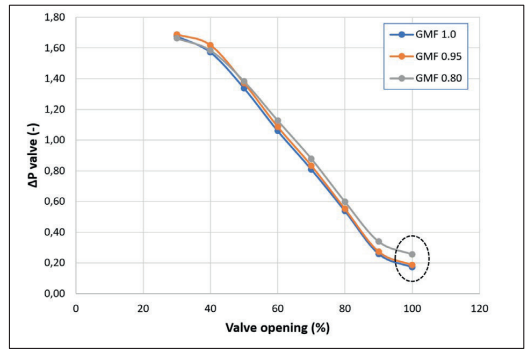

Figure 52: Valve differential pressure against valve opening

The liquid impact on the valve multiphase flow coefficient is shown in Figure 53. It can be seen that the flow coefficient decreases with increasing liquid content. The effect is most pronounced at high valve openings, where the valve flow rate decreases markedly, and the valve differential pressure increases drastically. At maximum valve opening, the flow coefficient at GMF 0.80 is reduced by 22.5% relative to dry conditions, which is expected to have a significant impact on the flow rate in wet conditions.

Thus, the previous scenario, «Gradual increase of liquid content», was rerun in the simulation model at high flow rates, with updated valve flow coefficient values. Although only the data at GMF 0.95 and GMF 0.80 are compatible between the two tests, Figure 54 shows a significantly improved correspondence between test and simulation (green triangles). This underlines that a complete understanding of the behavior of the entire compressor system in wet conditions is necessary to achieve accurate simulation results.

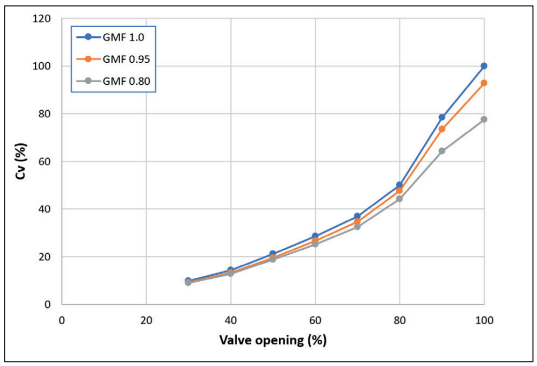

Figure 53: Multiphase valve flow coefficient

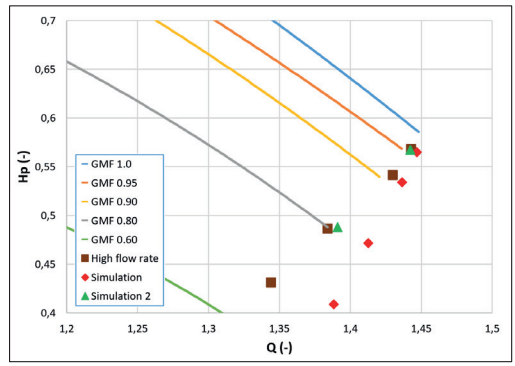

Figure 54: A stepwise increase of liquid content at high flow rates with - Test vs simulation

Summary and conclusion

The wet gas impact on the control valve performance has been studied and analyzed. Wet gas accounts for a higher differential pressure over the valve and a reduced flow rate. The combined effect is a marked reduction in the valve flow coefficient at reduced GMFs. Hence, wet gas alters not only alter the compressor performance, but also the system behavior. The combined effect is important to understand for development and operation of future wet gas compressor systems.

Driver trip in wet conditions results in a greater speed decrease owing to the higher total mass flow rate and hence the increased fluid power. Compared to dry conditions, a GMF of 0.80 results in a 30 % larger speed drop one second after trip initiation. The driver trip scenario was closely captured with the simulation model, in both dry and wet conditions.

The compressor operating point follows the steady state characteristics accurately when subjected to a stepwise increase of liquid content (GMF 1.0 to 0.70). Overall, the model provided a satisfactory match with the test points. Accounting for the valve performance in wet gas flow improved the simulation accuracy significantly, which underlines that a complete understanding of the system response in wet conditions is necessary to achieve accurate simulation results.

5.4 Digitalization of compressor systems

Digitalization is a topic which is eagerly discussed for many applications, including compressor systems. This section presents data from a real compressor trip. The investigation reveals that plant data alone may not be sufficient for analysis of the trip trajectory. Hence, the trip scenario was analyzed in light of both fan law principles and utilization of a detailed dynamic model. The results reveal that utilization of a dynamic model gives important insight into the compressor system dynamics during a trip. These findings form a basis for future digitalization of the plant. The idea will be developed into the specification of a concept called a *Digital Compressor*. The concept will also be relevant for subsea wet gas compression systems with limited instrumentation and stringent availability demands.

The export compressor is shown in Figure 55. The compressor is protected by both an anti-surge and a hot gas bypass system. The anti-surge control system ensures the correct surge margin during normal operation, but it is too slow to protect the compressor from the pressure transients during a trip. At trip, the hot gas bypass valve opens after a small initial delay (trip signal, solenoid and inherent valve delay) and is fully open less than one second after the trip signal initiation. Performance testing and performance deterioration due to both internal seal leakages and fouling are experienced. Therefore, yearly field performance testing of the compressors has been carried out, supplemented by computer-based performance predictions. Validation of the compressor trip trajectory at plant is of utmost importance to ensure stable and reliable operation of the export compressors during any operating and/or transient conditions. In addition, dynamic simulations have been used to ensure stable operation and tuning of control settings for both process and drive system.

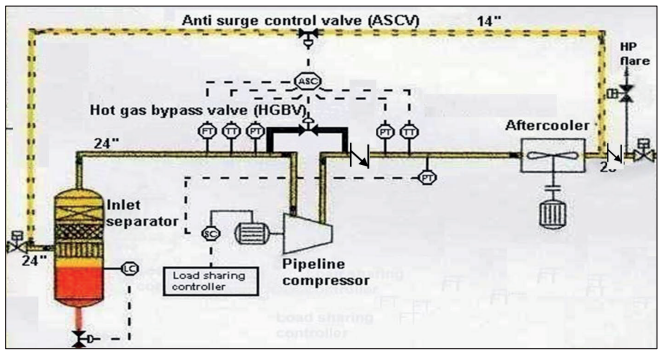

Figure 55: Export compressor system.

Figure 56 shows the compressor trip trajectory utilizing measured plant data. A few factors complicate the current analysis. First, there appears to be a significant delay on the flow measurement. After 500 ms the measured mass flow remains almost unchanged although the compressor speed has dropped from 6232 rpm to 5729 rpm. Second, the static discharge pressure reading is located downstream of the discharge check valve (see Figure 55), which inevitably will shut during a trip. Thus, as soon as the valve shuts the pressure reading no longer describes the compressor discharge pressure. The static discharge pressure is shown in Figure 57, where compressor trip is initiated at the 2.00 second time stamp. A sudden pressure drop is detected after 400 ms followed by distinct fluctuations. The trend however (dotted red line) reveals a close to constant discharge pressure after the drop, as expected after a check valve closes. This suggests that the check valve closes after approximately 400 ms. At 3.5 seconds the discharge pressure starts decreasing, which correlates with the acting of the anti-surge control system.

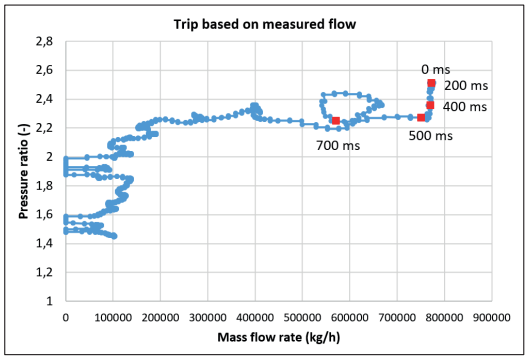

Figure 56: Trip based on measured flow and static pressure readings.

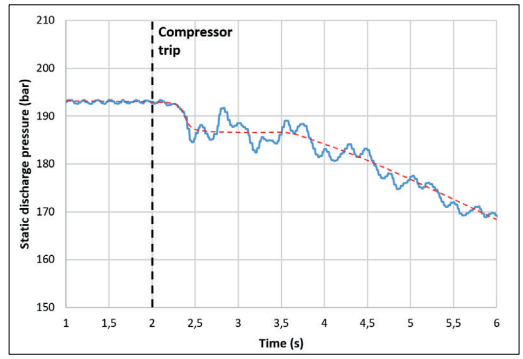

Figure 57: Static discharge pressure reading.

Due to the uncertainties concerning the flow measurement, the trip trajectory was reconstructed utilizing the compressor speed and compressor performance data. Knowing the compressor speed and polytropic head gives the volumetric flow rate by utilizing the established performance envelope. Fan law principles, with reference to the closest established speed line, were used to interpolate between the curves.

The new trip trajectory is shown in Figure 58. It can readily be seen that the flow rate declines while the polytropic head remains approximately constant after the first 300 ms. Shortly after 200 ms the hot gas bypass starts opening, with the purpose of preventing the compressor from surging. From 500 – 900 ms the effect of the closed check valve is evident, yielding a close to constant pressure ratio, hence giving the erroneous impression that the compressor is entering the surge region.

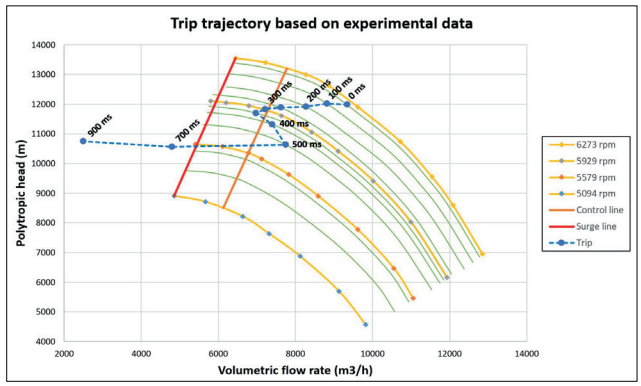

Figure 58: Trip trajectory based on measured compressor speed, static pressure readings and utilization of fan law principles.

This is a challenging case to analyze for several reasons. The discharge pressure reading is only usable as long as the discharge check valve is open, i.e. the first 400-500 ms. Additionally, the lack of information concerning the valve stem position means that both the valve behavior (fluttering etc.) and the exact time the valve closes are unknown. Furthermore, the flow device is installed within the anti-surge control loop (see Figure 55), meaning that the measured flow and the compressor inlet flow will not be equal as soon as the hot gas bypass system opens. Therefore, a dynamic simulation model was utilized to provide a better understanding of the system behavior during the trip.

Dynamic model results

The dynamic simulation model was tuned against the latest known plant data. The model was exposed to the same inlet conditions, revealing a close match with plant data. Figure 59 shows the simulated compressor rundown trajectory. The trip trajectory predicted by the model matches the first 400 ms of Figure 58 closely, confirming a turning point at 7000 m^3/h. More importantly, the model predicts that the compressor will remain in the stable part of the characteristics during the trip. Figure 60 shows a close match between the measured and simulated compressor speed.

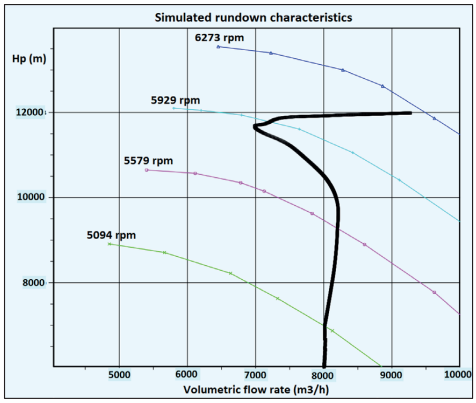

Figure 59: Simulated rundown trajectory.

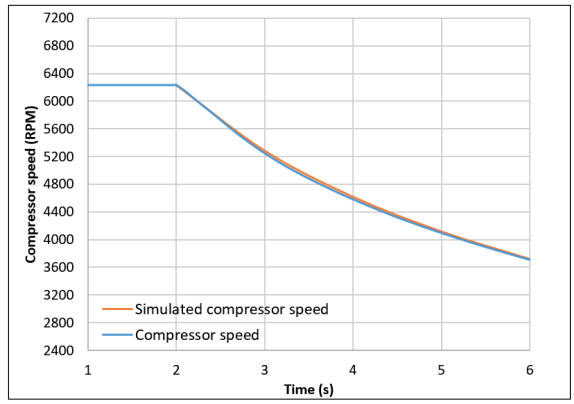

Figure 60: Measured vs simulated compressor speed during rundown.

Figure 61 shows the measured mass flow in relation to the simulated mass flow. The latter describes the mass flow at the exact location of the flow measurement device and must not be mistaken for the compressor mass flow. In contrast to the measurement, the simulation reveals negative mass flow after the hot gas bypass system starts acting. This indicates that the flow calculation or the measured differential pressure only provides positive readings/calculations regardless of flow direction. This argument is strengthened if one subtracts the

time delay of the flow measurement device while changing the sign for the measured mass flow at the same time stamp as the simulated mass flow becomes negative. This is shown with the dotted curve in Figure 62, revealing a close match between the two.

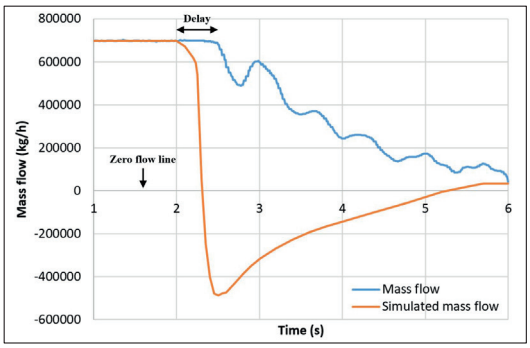

Figure 61: Measured vs simulated mass flow rate.

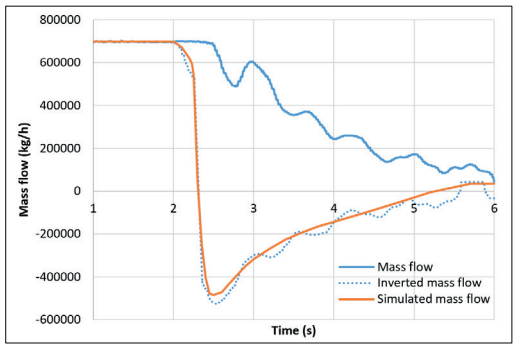

Figure 62: Measured vs simulated mass flow when accounting for time delay and sign conversion.

For the further development of the results and ideas presented here, a laboratory set up is being prepared as illustrated in Figure 63. The NTNU compressor rig is instrumented with a diversity of sensors more accurate than those found at typical compressor facilities. This allows for experimenting with the sensor inputs fed to the simulator: what is the minimum viable instrumentation - in terms of which sensors, what accuracy and what sampling rates are required. The laboratory compressor can be modified with degraded performance, variable molecular weight, sensor offsets and failures, etc. For the latter case, it will be relevant to investigate fault-tolerant scenarios where a simulator output (soft sensor) can replace the failed sensor measurement. Detecting compressor degradation, especially when compressor curves flatten out and the stability margin is reduced, may be crucial to safe and economical plant operation. Furthermore, the idea is that the simulation model will run in parallel with the process providing live data on: Compressor performance, safety margins, measurement accuracy/delays and calculation of parameters which are not measured. The concept will also be relevant for subsea wet gas compression systems with limited instrumentation and stringent availability demands.

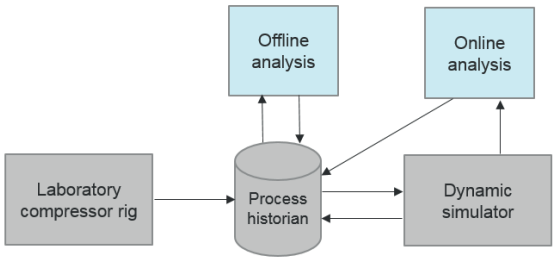

Figure 63: Laboratory setup for future digital analysis.

Summary and conclusion

The current case sheds light on challenges regarding transient analysis on a full-scale export compressor system owing to time resolution, synchronization and instrumentation placement. Utilization of a detailed dynamic model recreated the trip scenario and showed a close correlation with the experimental data. The model predicted that the compressor did not surge during trip, as was confirmed by compressor vibrational analysis.

Utilization of an accurate dynamic model proved to be a valuable tool to visualize the trip trajectory and thereby provide key information for tuning of the compressor safety system. Direct comparison between plant variables and simulated variables gave valuable insight on possible delays and trends. The results presented

here form the foundation for development of a concept *digital compressor*. In short, this is a simulation model that will run in parallel with the process to provide live data on:

- Compressor performance and degradation
- Compressor safety margins
- Measurement offset and failures
- Event-based analysis (Driver trip, change in operating conditions, operation of several compressor trains etc.)

6 CONCLUSION

The current work includes both experimental research and model simulation on transient behavior of wet gas compression systems. The experimental work forms a basis for model simulation and validation. The main results and conclusions are:

- The interaction between the impeller, diffuser and volute is vital to understand with respect to compressor hysteresis. At low flow rates the segregated liquid swirls along the volute wall and re-enters the diffuser. Depending on the volute flow direction (HS or SH) and its interaction with the diffuser, a distinct impact on performance and stability was documented. Narrowing the diffuser width, i.e. increasing the radial diffuser velocity, improved the compressor performance and eliminated the volute flow influence on compressor performance. Care should be taken when it comes to utilizing established dry gas compressor design for wet gas compressors.

- The pressure ratio increases and the polytropic efficiency decreases when the compressor is subjected to wet gas flow. Care should be taken when analyzing stability and surge margins at different GMFs. Increased liquid content reduces both the polytropic head and "head rise to surge", while the "pressure rise to surge" remains, providing a satisfactory stability margin. Establishment of accurate and repeatable wet gas performance data is paramount, as it forms a necessary basis for model simulation

- The compressor performance has been analyzed when subjected to inlet slugs down to a GMF of 0.185, which had a marked impact on the gas flow rate, compressor shaft torque and compressor pressure ratio. Subsea compressor systems may suffer from large variations in GMF that may arise during start-up or when entering tail production of an oil and gas field. A slow pressure response and limited available power may result in compressor surge and trip.

- The wet gas impact on the control valve performance has been studied and analyzed. Wet gas accounts for a higher differential pressure over the valve and a reduced flow rate. The combined effect is a marked reduction in the valve flow coefficient at reduced GMFs. Hence, wet gas alters not only the compressor performance, but also the system behavior. The combined effect is important to understand for development and operation of future wet gas compressor systems.

- A dynamic simulation model has been built and tuned to replicate the wet gas compressor test facility at NTNU. The model includes all relevant mechanical and process data. In cooperation with Aspentech R&D, Hysys Dynamics has been extended to support modeling of wet gas compressors. This enables the user to input multiple performance curves at different GMFs as well as different compressor speeds. In addition, the user has the possibility to input multiple surge and stonewall curves based on the GMF.

- The simulation model provided a close correspondence to the transient test cases. Driver trip in wet conditions resulted in a greater speed decrease owing to the higher total mass flow rate and the increased fluid power. Compared to dry conditions, a GMF of 0.80 resulted in a 30 % larger speed drop. The model provided a satisfactory match against the experimental operating points, when subjected to a gradual increase of liquid content (GMF 1.0 to 0.70). Accounting for the valve performance in wet gas flow improved the simulation accuracy significantly, which underlines that a complete understanding of the system response in wet conditions is necessary to achieve accurate simulation results.

- A linear interpolation is performed when operating at GMFs between the provided performance curves, within the simulation model. The methodology has been validated against both hydrocarbon and air/water performance data, within a GMF range of 1.0 to 0.8. The methodology has proved to be applicable and provided accurate results, i.e. less than 3.5% deviation in terms of polytropic head and efficiency.

- Striking similarities have been documented regarding compressor performance scaling in wet gas versus dry gas. The results reveal that the compressor scales in a similar manner regardless of GMF. That is, the slope (dPr/dQ) is hardly affected by the GMF and the relative position between the dry and wet operating points remain close to constant as the speed increases. The affinity laws match the experimental results well for all tested GMFs. No major difference can be detected regarding the accuracy of the affinity laws in dry gas versus wet gas flow. Thus, the affinity laws have proven to be applicable to wet gas flow for the current application, i.e. a single-stage compressor operating at ambient conditions.

- Utilization of a detailed dynamic simulation model provided important insight into the compressor dynamics during a driver trip of an export compressor system. The results from this case will be developed further into a concept called *digital compressor*. In short, this is a simulation model that will run in parallel with the process to provide live data on:
    - Compressor performance and degradation
    - Compressor safety margins
    - Measurement offset and failures
    - Event-based analysis (Driver trip, change in operating conditions, operation of several compressor trains etc.)

7 FURTHER WORK

Continued studies should involve the influence of different multiphase flow characteristics on the compressor and system performance. Further studies on flow behavior through the impeller and diffuser would also be of great interest, and potentially give insight into new design principles. Based on my work a redesign of the volute is suggested to physically remove the possibility of volute backflow.

More studies are necessary to continue development of wet gas compressor modeling, i.e additional parameters like the fluid density ratio, are needed to accommodate the performance shift related to changes in composition and inlet conditions. Finally, emphasis should be given to system behavior and system response to contribute to design and operation of future subsea production systems.

REFERENCES

[1] Norwegian Petroleum Directorate, Resource report 2017, www.ndp.no.

[2] www.norskpetroleum.no, data from the Norwegian Petroleum Directorate.

[3] L. Brenne, T. Bjørge, L. E. Bakken, Ø. Hundseid, “Prospects for Sub Sea Wet Gas Compression”, ASME Turbo Expo 2008, GT2008-51158.

[4] D. Müller-Link, J. U. Brandt, M. Reichwage, G. Schröder, “Wet Gas Compression – A logical Step to Follow Multiphase Boosting”, SPE 2002, SPE 78556.

[5] T. W. Knudsen, N. A. Sølvik, “World First Submerged Testing of Subsea Wet Gas Compressor”, OTC 2011, OTC21346.

[6] G. Kleynhans, L. Brenne, S. Kibsgaard, P. Dentu, “Development and Qualification of a Subsea Compressor”, OTC 2016, OTC-27160-MS, Texas.

[7] ISO10493, “Axial and centrifugal compressors and expander-compressors”, 2015.

[8] API Standard 617 – Axial and Centrifugal Compressors and Expander-compressors, 8th edition, 2014.

[9] ASME PTC 10-1997, “Performance test code on compressors and exhausters”, American Society of Mechanical Engineers

[10] Ø. Hundseid, L. E. Bakken, “Integrated wet gas compressor test facility”, ASME Turbo Expo 2015, GT2015-43004

[11] L. Brenne, T. Bjørge, J. Gilarranz, J. Koch and H. Miller: “Performance Evaluation of a Centrifugal Compressor Operating Under Wet Gas Conditions”, Proceedings of the 34th Turbomachinery symposium, 2005.

[12] M. Bertoneri, S. Duni, D. Ransom, L. Podesta, M. Camatti, M. Bigi, M. Wilcox, “Measured performance of a two-stage centrifugal compressor under wet conditions”, ASME Turbo Expo 2012, GT2012-69819, Denmark.

[13] Ø. Hundseid, L.E. Bakken, T. G. Grüner, L. Brenne, T. Bjørge, ”Wet gas performance of a single stage centrifugal compressor”, ASME Turbo Expo 2008, GT2008-51156

[14] M. Fabbrizzi, C. Cerretelli, F. Del Medico, M. D’Orazio “An Experimental Investigation of a Single Stage Wet Gas Centrifugal Compressor”, ASME Turbo Expo 2009, GT2009-59548, Florida, USA.

[15] R. M. Ramberg, L.E. Bakken, “Influence of Visous Fluids on Multiphase Pump Performance”, ASME FEDSM 1998, FEDSM98-4869.

[16] L. Brenne, T. Bjørge, L. E. Bakken,” Pressure recovery of an air-water annular flow through a straight-walled diffuser”

[17] R. J. McKee, A.G. Hernandez, “Simulation of Centrifugal Compressor Trips for Surge Avoidance System design”, Pipeline Simulation Interest Group, 2003

[18] G.B Tveit, L.E. Bakken, T. Bjørge, “COMPRESSOR PERFORMANCE IMPACT ON RUNDOWN CHARACTERISTICS”, European Turbomachinery Conferense, 2005.

[19] G.B Tveit, L.E. Bakken, T. Bjørge, “COMPRESSOR TRANSIENT BEHAVIOR”, ASME Turbo Expo 2004, GT2004-53700.

[20] B. Stoffel, "Experimentelle Untersuchung zur raumlichen und zeitlichen Struktur der Teillast-Rezirkulationen bei Kreiselpumpen," Forschung im Ingenieurwesen, 55 (5), 1989.

[21] K. A. Kaupert, T. Staubli, “The Unsteady Pressure Field in a High Specific Speed Centrifugal Pump Impeller— Part II: Transient Hysteresis in the Characteristic”, Transactions of ASME, Journal of Fluids Engineering, 121 pp. 627-632, 1999.

[22] P. Hergt, J. Starke, “Flow patterns causing instabilities in the performance curves of centrifugal pumps with vaned diffusers”, Proceeding of the second international pump symposium, pp. 67-76, 1985.

[23] W. H. Fraser, "Flow Recirculation in Centrifugal Pumps," Proceeding of the tenth turbomachinery symposium, pp. 95-100, 1982

[24] I. J. Day, E. M. Greitzer, N. A. Cumpsty, “Prediction of Compressor Performance in Rotating Stall”, Transactions of ASME, Journal of Engineering for Power, 100 pp. 1-12, 1978.

[25] J. M. Schultz, “The Polytropic Analysis of Centrifugal Compressors”, Journal of Engineering for Power, 1962.

[26] IEC 60534-2-1 International Standard – Industrial process control valves part 2-1: Flow Capacity – Sizing equation for fluid flow under installed conditions.

[27] R. Darby, P. Meiller, J. Stockton, “Select the best model for two-phase relief sizing”, Chemical Engineering Progress, 2001

[28] J. Schmidt, “Sizing of nozzles, venturis, orifices, control and safety valves for initiall sub-cooled gas/liquid two phase flow – The HNE-DS method”, Forsch Ingenieurwes, 2007.

[29] V. Ferrara, L. E. Bakken, “Wet Gas Compressor Surge Stability”, ASME Turbo Expo, GT2015-42650, Montreal, 2015.

[30] V. Ferrara, L. E. Bakken, S. Falomi, G. Sassanelli, M. Bertoneri, A. S del Greco, “WET COMPRESSION: PERFORMANCE TEST OF A 3D IMPELLER AND VALIDATION OF PREDICTIVE MODEL”, ASME Turbo Expo 2016, GT2016-57976

[31] M. Bakken, T. Bjørge, “Volute Flow Influence on Wet Gas Compressor Performance”, ASME Gas Turbine Conference and Exhibition, GTIndia2017-4529.

[32] E. M. Greitzer, “Surge and Rotating Stall in Axial Flow Compressors – Part 1: Theoretical Compression System Model”, ASME Journal of Engineering for Power, 1976.

PAPER I

Is not included due to copyright restrictions

PAPER II

Is not included due to copyright restrictions

PAPER III

Is not included due to copyright restrictions

PAPER IV

Is not included due to copyright restrictions

PAPER V

Is not included due to copyright restrictions

PAPER VI

Is not included due to copyright restrictions

PAPER VII

Is not included due to copyright restrictions